NICOLÁS CÉSPEDES CÁRDENAS

Analysis of static and temporal trade animal network for evaluation of simulation of disease quality

São Paulo
2020

NICOLÁS CÉSPEDES CÁRDENAS

Analysis of static and temporal trade animal network for evaluation of simulation of disease quality

Thesis submitted to the Postgraduate Program in Experimental Epidemiology applied to Zoonoses of the School of Veterinary Medicine and Animal Science of the University of São Paulo to obtain the Doctor's degree in Sciences.

Department:

Department of Preventive Veterinary Medicine and Animal Health

Area:

Experimental Epidemiology applied to Zoonoses

Advisor:

Prof. José Henrique Hildebrand Grisi Filho, Ph.D.

São Paulo

2020

DADOS INTERNACIONAIS DE CATALOGAÇÃO NA PUBLICAÇÃO

(Biblioteca Virginie Buff D'Ápice da Faculdade de Medicina Veterinária e Zootecnia da Universidade de São Paulo)

T. 3992
FMVZ

Céspedes Cárdenas, Nicolás
Analysis of static and temporal trade animal network for evaluation of simulation of disease quality / Nicolás Céspedes Cárdenas. – 2020.
86 f. : il.

Título traduzido: Análise de redes estáticas e temporais de trânsito animal para avaliar a qualidade das simulações de doença.

Tese (Doutorado) – Universidade de São Paulo. Faculdade de Medicina Veterinária e Zootecnia. Departamento de Medicina Veterinária Preventiva e Saúde Animal, São Paulo, 2020.

Programa de Pós-Graduação: Epidemiologia Experimental Aplicada às Zoonoses.
Área de concentração: Epidemiologia Experimental Aplicada às Zoonoses.
Orientador: Prof. Dr. José Henrique Hildebrand Grisi Filho.

1. Análise de redes. 2. Vigilância animal. 3. Epidemiologia. 4. Modelos de espalhamento. I. Título.

Ficha catalográfica elaborada pela bibliotecária Maria Aparecida Laet, CRB 5673-8, da FMVZ/USP.

Comissão de Ética no Uso de Animais
Faculdade de Medicina Veterinária e Zootecnia
Universidade de São Paulo

São Paulo, 6th November 2020

CERTIFIED

We certify that the Research "Analysis of static and temporal trade animal network for evaluation of simulation of disease quality", protocol number CEUAx 6601021216 (ID 000693), under the responsibility José Henrique De Hildebrand E Grisi Filho, agree with Ethical Principles in Animal Research adopted by Ethic Committee in the Use of Animals of School of Veterinary Medicine and Animal Science (University of São Paulo), and was approved in the meeting of day April 06, 2017.

Certificamos que o protocolo do Projeto de Pesquisa intitulado "Analise de redes estáticas e temporais de transito animal para avaliar a qualidade das simulações de doença", protocolado sob o CEUAx nº 6601021216, sob a responsabilidade de José Henrique De Hildebrand E Grisi Filho, está de acordo com os princípios éticos de experimentação animal da Comissão de Ética no Uso de Animais da Faculdade de Medicina Veterinária e Zootecnia da Universidade de São Paulo, e foi aprovado na reunião de 06 de abril de 2017.

Prof. Dr. Marcelo Bahia Labruna
Coordenador da Comissão de Ética no Uso de Animais
Faculdade de Medicina Veterinária e Zootecnia da Universidade de São Paulo

Camilla Mota Mendes
Vice-Coordenador
Faculdade de Medicina Veterinária e Zootecnia da Universidade de São Paulo

EVALUATION FORM

Author: CÁRDENAS, NICOLÁS CÉSPEDES

Title: **Analysis of static and temporal trade animal network for evaluation of simulation of disease quality**

Thesis submitted to the Postgraduate Program in Experimental Epidemiology applied to Zoonoses of the School of Veterinary Medicine and Animal Science of the University of São Paulo to obtain the Doctor's degree in Sciences.

Date: _____/_____/_____

Committee Members

Prof. _____

Institution:_____ Decision: _____

Prof. _____

Institution: _____ Decision: _____

Prof. _____

Institution: _____ Decision: _____

Prof. _____

Institution:_____ Decision: _____

Prof. _____

Institution:_____ Decision: _____

ACKNOWLEDGEMENTS

I am really grateful to so many people and institutions that make me grow up at all levels in my life over these years. To my best example in life my mom (MUCHAS GRACIAS MA), to all members of my family that I miss so much. To the LEB professors, starting with my advisor José Henrique Hildebrand Grisi Filho very thanks for your support, Marcos Amaku, Fernando Ferreira, Ricardo Dias and Owaldo Baquero all of them amazing teachers and epidemiologists. Many thanks to Kim VanderWall from University of Minnesota, Julio Alvarez from the Universidad Complutense and, Gustavo Machado from NCS University for the discussions and the advices I've really learned so much from all you.

To my lab mattes friends Jason (el Jason) thanks for your patience and teaching me R when I barely knew how to load an excel table, very thanks Daniel (Matungo), Alfredito, Anita Perolita, Germana, Ligia, Guilherme, Gisella, João, Juliana, Maira, Choco, Sussai, Bia; thanks to friends who have accompanied me in this doctorate Eliana, Carlos, Andre, Nelson, Jessica, Hellen, Sandy; many thanks for the memorable and also for the stupid moments; Damaris thanks for the wonderful travels, conversations and views, thanks Dona Claudia for the support, all of you are my family in Sao Paulo. To the epigroup: Pilar, Clara, Vicent, Kendy and also friends in Madrid: Irene (not by the coffee with ice), Pedro, Javi (for all napos de choco), Thanks to Natalia and her amazing family.

Very special thanks to Giuliana Barajas for all figures and design and illustrations help, I always felt calm and happy by your side. At this point I realized that there are many people so I am going to place their names in this "word search", if you don't find your name it's your fault! and not because my memory has failed.

Thanks to the department' secretary, workers and professors from **VPS** for the help given to me in these years.

Acknowledgments for all institution and programs that support this work over those years. ***Department of Veterinary Population Medicine***, **University of Minnesota**, MN, United States. ***VISAVET Health Surveillance Centre***, **Universidad Complutense de Madrid**, Madrid, Spain. *Ministério Agricultura, Pecuária e Abastecimento* (**MAPA**), *Companhia Integrada de Desenvolvimento Agrícola de Santa Catarina* (**CIDASC**), Santa catarina, Brazil, and Secretary of Agriculture, Livestock and Agribusiness of Rio Grande do Sul State (**SEAPA-RS**), Porto Alegre, Brazil. Thanks for economic support to the Coordenação de Aperfeiçoamento de Pessoal de Nível Superior - Brasil **(CAPES) - Finance Code 001** and the scholarship period at Universidad Complutense de Madrid, sponsored by the **CAPES (grant n. 88887.373827/2019-00).**

RESUMO

CESPEDES CARDENAS, N. **Análise de redes estáticas e temporais de trânsito animal para avaliar a qualidade das simulações de doença**. [Analysis of static and temporal trade animal network for evaluation of simulation of disease quality]. 2020. 86 p. Tese (Doutorado em Ciências) – Faculdade de Medicina Veterinária e Zootecnia, Universidade de São Paulo, São Paulo, 2020.

A análise de rede sociais (SNA) é uma ferramenta poderosa para descrever o impacto do comércio de animais na disseminação de patógenos, e gerar padrões essenciais que podem ser usados para entender, prevenir e mitigar possíveis surtos.

Este estudo teve como objetivos descrever e analisar as redes de movimentação animal entre propriedades de suínos do estado de Santa Catarina (SC) e bovinos do estado do Rio Grande do Sul (RS), para dirigir a vigilância de doenças transmitidas por contato baseado nas interações entre as propriedades (granjas e fazendas), utilizando diversos modelos de espalhamento de doença com objetivos específicos para cada estado. Para o estado de SC foi descrita a rede estática e temporal, foram calculadas as comunidades internas de comércio, e a efetividade das ações de controle através de análises de cadeias de contato. Baseado nessas informações, foram propostos dois índices no nível de municípios para classificá-los de acordo com a sua participação na rede. Para o estado do RS foi descrita a rede estática e temporal de transporte de bovinos e bubalinos e os tipos de componentes conectados da rede. Um modelo de espalhamento Susceptível-Oculto-Reativo-Infeccioso (SORI) foi implementado para representar a dinâmica da tuberculose bovina (TB) na população, adicionalmente, foram testadas ações de controle utilizando o modelo proposto.

Os resultados mostraram redes altamente conectadas e com dinâmicas temporais e espaciais bem definidas. Os modelos de simulação demostraram que é possível reduzir tamanhos de surtos epidêmicos, selecionando estrategicamente propriedades, baseado em métricas de SNA como "*degree*" e "*betweenness*". Estas informações são importantes para o direcionamento de sistemas da vigilância de doenças infeciosas baseada no risco.

Palavras-chave: Analise de redes. Vigilância animal. Epidemiologia. Modelos de espalhamento.

ABSTRACT

CESPEDES CARDENAS, N. **Analysis of static and temporal trade animal network for evaluation of simulation of disease quality**. 2020. 86p. Tese (Doutorado em Ciências) – Faculdade de Medicina Veterinária e Zootecnia, Universidade de São Paulo, São Paulo, 2020.

Social network analysis (SNA) is a powerful tool to describe the impact of the animal trade on the spread of pathogens, and to generate essential patterns that can be used to understand, prevent and mitigate possible outbreaks.

This study aimed to describe and analyze animal movement networks between pig properties in the state of Santa Catarina (SC) and cattle in the state of Rio Grande do Sul (RS), to guide the surveillance of diseases transmitted by contact based on interactions between properties (farms and farms), using different models of disease spread with specific objectives for each state. For the state of SC the static and temporal network was described, the internal communities of commerce were calculated, and the effectiveness of control actions through analysis of contact chains. Based on this information, two indexes were proposed at the municipal level to classify them according to their participation in the network. For the state of RS, the static and temporal transport network of cattle and buffaloes and the types of connected components of the network were described. A Susceptible-Occult-Reactive-Infectious scattering model (SORI) was implemented to represent the dynamics of bovine tuberculosis (TB) in the population, in addition, control actions were tested using the proposed model. The results showed highly connected networks with well-defined temporal and spatial dynamics. The simulation models demonstrated that it is possible to reduce the size of epidemic outbreaks, strategically selecting properties, based on SNA metrics such as "degree" and "betweenness". This information is important for targeting risk-based infectious disease surveillance systems

Keywords: Network analysis. Animal surveillance. Epidemiology. spread disease models.

SUMMARY

INTRODUCTION

This work consists of two chapters related to network analysis in preventive veterinary medicine. Throughout this manuscript, different network approaches will be described showing their advantages and disadvantages. Each chapter is in a classic scientific article format and each section (introduction, material and methods, results, discussion and references) will be exclusive for each chapter.

In the first chapter we focus on the analysis of the pig trade network in the state of Santa Catarina, the static and temporal network was described, the internal communities of commerce were calculated, and the effectiveness of control actions through analysis of contact chains. Based on this information, two indexes were proposed at the municipal level to classify them according to their participation in the network.

The cattle trade network and tuberculosis spread were the object of study in the second chapter, here, the static and temporal network trade and the types of connected components of the network were described. A multiscale Susceptible-Occult-Reactive-Infectious scattering model (SORI) was implemented to represent the dynamics of bovine tuberculosis (TB) in the population, additionally, control actions were tested using the proposed model using interventions planned according to metrics of network analysis.

CHAPTER 1

SPATIO-TEMPORAL NETWORK ANALYSIS OF PIG TRADE TO INFORM THE DESIGN OF RISK-BASED DISEASE SURVEILLANCE

Abstract

Network analysis is a powerful tool to describe, estimate, and predict the role of pig trade in the spread of pathogens and generate essential patterns that can be used to understand, prevent, and mitigate possible outbreaks. This study aimed to describe the network of between-farm pig movements and identify heterogeneities in the connectivity of premises in the state of Santa Catarina, Brazil, using social network analysis (SNA). We used static and temporal network approaches to describe pig trade in the state by quantifying network attributes using SNA parameters, such as causal fidelity, loyalty, the proportion of node-loyalty, resilience of outgoing contact chains, and communities. Two indexes were implemented, the first one is a normalized index based on SNA-farm level measures and other index-based SNA-farm level measures considering the swine herd population size from all premises, both indexes were summarized by municipality to target and rank surveillance activities. Within Santa Catarina, the southwest region played a key role in that 80% of trade was concentrated in this region, and thus acted as a hub in the network. In addition, nine communities were found. The results also showed that premises were highly connected in the static network, with the network exhibiting low levels of fragmentation and loyalty. Also, just 11% of the paths in the static network existed in the temporal network which accounted for the order in which edges occurred. Therefore, the use of time-respecting-paths was essential to not overestimate potential transmission pathways and outbreak sizes. Compared to static networks, the application of temporal network approaches was more suitable to capture the dynamics of pig trade and should be used to inform the design of risk-based disease surveillance.

1. INTRODUCTION

Infectious diseases in livestock cause great economic losses, block international trade, compromise animal welfare, reduce productivity, and induce large costs through disease control and eradication (BAJARDI et al., 2012; MOSLONKA-LEFEBVRE et al., 2016). In Brazil, the swine industry consists of approximately two million sows and produced 3.76 million tons of meat in 2018, which has made Brazil the fourth-largest producer of pork in the world. Within Brazil, the state of Santa Catarina (SC) is the largest swine producer (EMBRAPA, 2019). The control of infectious diseases is critical

to maintaining this leadership, and the movement of animals through trade plays an important role in spreading infectious diseases (SCHULZ et al., 2017).

In recent years, the Brazilian National Veterinary Services (BNVS) has intensified disease surveillance, control, and eradication efforts. Until 2019, SC is the only state in the country free of foot-and-mouth disease (FMD) without vaccination. Therefore, it is critical to understand patterns and risks associated with animal movements to maintain this disease-free status. This is especially relevant for the national efforts to transition from the country-wide status of FMD disease-free with vaccination to without vaccination, which is expected to be achieved by 2023 (MAPA, 2017). In this context, the analysis of contact networks is a powerful tool to describe, predict and estimate the role of trade in the spread of diseases (LEBL et al., 2016; VANDERWAAL et al., 2016a), producing important data to understand, prevent, and mitigate possible outbreaks in the region.

Much of the research on livestock movement networks has used static representations of networks, which assumes that connections among farms are constant and unchanging through time. However, static representations over-represent the network's connectivity (LENTZ; SELHORST; SOKOLOV, 2013). Temporal representations of networks consider the active and inactive connections according to a time interval, which is a more accurate characterization of network patterns (BÜTTNER; SALAU; KRIETER, 2016; CHATERS et al., 2019).

The objective of this study was to characterize the dynamics of pig trade, describe both static and temporal movement networks, and provide useful information to target surveillance actions in municipalities and individual premises in the state of Santa Catarina, Brazil, according to their importance in the network. Such rankings, which are based on different parameters derived through social network analysis (SNA), helps to improve the prevention, control, and eradication of communicable diseases spread through animal movements.

2. MATERIAL AND METHODS

2.1 Data

Records of animal movements from Santa Catarina (SC) state in Brazil were provided by the official veterinary service in this state. The database includes the movements of pigs in SC in Brazil from 2015-01-01 to 2017-12-31. Records included all intra-state movements as well as outgoing movements with destinations outside of SC. Records with errors about the origin, destination, date or movements with destinations outside of SC were removed prior to any analysis. For the network analysis, movements with the purpose of slaughter were excluded, which were assumed to be epidemiological endpoints.

2.2 Trade description

Premises that moved at least once during the study period were included as nodes in the network; premises for which no movements were recorded were assumed to be inactive. In order to represent the spatial distribution of premises, the number of premises was grouped by geolocation across a ~3km^2 grid (see figure 1). The production type of each premises was classified according to the records provided by the official surveillance veterinary service. Eight type of premises were classified: Finishers (n = 7119), Breeding-farms (n = 2255), Non-commercial or backyard farms (n= 2055), Nursery farms (n = 1398), Wean-to-finisher & mixed farms (n= 447), Slaughterhouses (n=189), Certified-Swine-Breeder-Farms (n = 138), and others premises (n=111).

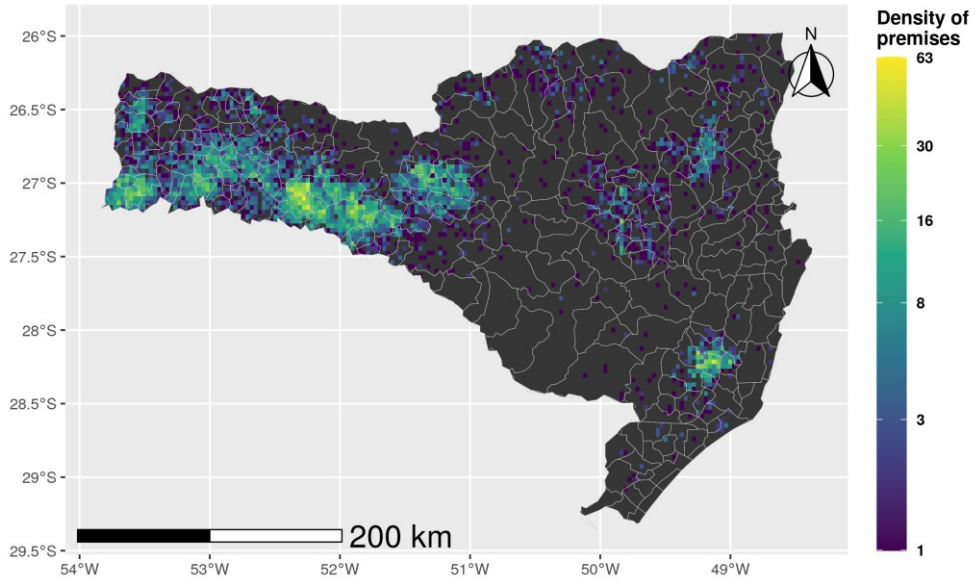

Figure 1. The study area included the state of Santa Catarina, Brazil. A 3km^2 grid was projected onto the map, the density of premises was represented as the number of premises allocated in each grid cell. The black background represents grids without premises. The gray lines represent the municipalities of SC.

In general, *Wean-to-finisher & mixed* premises house breeding sows and bores for the production of piglets, which are also fattened on premise for slaughter. This classification also included instances in which premises with more than one type of classification were co-located i.e. farrowing farms and farrow-to-finishing farms. *Breeding-farms* are premises which deliver piglets to nursery farms and, less frequently, to finishers. *Certified-Swine-Breeder-Farm (CSBF)* are premises with an official certificate to send animals for breeding purposes. *Non-commercial* farms are backyards farms and/or places where subsistence pig farming occurs. *Nurseries* are a type of premises designed specifically to house newly weaned pigs until they reach the grower/finisher stage. *Finishing* premises receive piglets from the farrowing farms and deliver fattening pigs to the slaughterhouses. *Other premises* are those that cannot be incorporated in the previous classification, such as pig events trade, laboratories, or without information.

Movements (including movements with destination to slaughterhouses) to and from different types of premises were analyzed and the number and percentage of movements and total of animals moved were summarized. The number of records by

purpose and their state destination (SC and the other Brazilian states) are shown in table 1.

Table 1. Total records and percentage by destination intra- and inter-SC State in Brazil.

Purpose of the Movement	Santa Catarina		Outgoing movements to outside SC	
	Total of records	% of records	Total of records	% of records
Slaughter	435.217	57,56	41.044	64,69
Fattening	254.394	33,65	12.224	19,27
Reproduction	66.080	8,74	10.146	15,99
Others	380	0,05	36	0,06
Total	756,071	100,00	63,450	100,00

2.3 Static network

We constructed contact networks in which premises were defined as nodes and movements between premises were considered edges. The consequent contact network g was based on the movements during the study and was represented as directed ($g_{ij} \neq g_{ji}$), such that where the origin (node i) and destination (node j) have a specific direction. We described the static network using data from all years of study as well as by year. Parameters that we measured are summarized in Table 2.

Table 2. Description of network analysis terminology and metrics

Parameter	Definition	Reference
Nodes	The unit of interest in network analysis, for example, herds or municipalities.	(WASSERMAN; FAUST, 1994)
Edge	Link between two nodes in the network.	
Degree (k)	Number of unique contacts to and from a specific node (e.g., farm location). When the direction is considered, the ingoing and outgoing contacts are separated: out-degree is the number of contacts originating from a specific node, and in-degree is the number of contacts coming into a specific node.	
PageRank	Google PageRank measure, a link analysis algorithm that produces a ranking of importance for all nodes in a network with a range of values between zero and one. The PageRank calculation considers the indegree of a given premises and the indegree of its neighbors.	(BRIN; PAGE, 1998)

Reverse of PageRank (rev(PageRank))	The Google PageRank algorithm can be typically implemented in an adjacent matrix $\mathbf{A}$ as a representation of the directed graph g. Here, we use a transposed adjacency matrix $\boldsymbol{t}(\mathbf{A})$ where $\boldsymbol{t}(\boldsymbol{A})\boldsymbol{ij} = \mathbf{1}$ if there exists an edge between the origin node $\boldsymbol{i}$ and destination node $\boldsymbol{j}$, otherwise $\boldsymbol{t}(\boldsymbol{A})\boldsymbol{ij} = \mathbf{0}$ if the edge does not exist. We then applied the PageRank algorithm using the $\boldsymbol{t}(\boldsymbol{A})$ to obtain the rev(PageRank).	
In/out Closeness centrality	Closeness centrality measures how many steps are required to access every other vertex from a given node; this measure can be calculated for incoming or outgoing paths.	(FREEMAN, 1978)
Betweenness	Describes the extent to which a node lies on paths connecting other pairs of nodes, defined by the number of geodesics (shortest paths) going through a node.	
In/out degree centralization	Quantifies the extent to which a minority of the farms are responsible for a majority of the incoming/outgoing movements.	(WASSERMAN; FAUST, 1994)
Clustering coefficient	Measures the degree to which nodes in a network tend to cluster together (i.e., if A → B and B → C, what is the probability that A → C), with a range of values between zero and one.	(WATTS; STROGATZ, 1998)
Giant weakly connected component (GWCC)	Proportion of nodes that are connected in the largest component when directionality of movement is ignored	(WASSERMAN; FAUST, 1994)
Giant strongly connected component (GSCC).	Proportion of the nodes that are connected in the largest component when directionality of movement is considered	(WASSERMAN; FAUST, 1994)

2.4 Fragmentation of the network

We computed the fragmentation F of the static network, which measures the proportion of pairs of nodes for which no connecting path exists (no direct or indirect connections between premises). The value can be calculated through an assessment of the number and size of components in the network, where a connected component C is defined as a subset of nodes V, where $C \subseteq V$ for which a path exists between any pair of nodes in C. Thus, fragmentation was calculated as:

$$F = 1 - \frac{\sum_k \quad S_k(S_k - 1)}{n(n-1)}, \tag{1}$$

Where S_k is the number of premises in component ***k*** and ***n*** the total number of premises in the network. Fragmentation ranges between zero and one. A value close to zero indicates a very connected network and a value of one means that every node is isolated (BORGATTI, 2006; SCHULZ et al., 2017).

2.5 Loyalty and node-loyalty of the network

We measured the proportion of preserved edges (θ) of a given premises between two consecutive years, $t-1$ and t, for the entire network. In order to quantify $\theta_i^{t-1,t}$, we define Y_i^{t-1}as the set of edges from a premises i in the time $t-1$ and Y_i^t as the set of edges from a premises i at time t. Then, $\theta_i^{t-1,t}$is given by the Jaccard Index in equation 2 (VALDANO et al., 2015; SCHULZ et al., 2017).

$$\text{edge loyalty} = \theta_i^{t-1,t} = \frac{|Y_i^{t-1} \cap Y_i^t|}{|Y_i^{t-1} \cup Y_i^t|} \tag{2}$$

The Jaccard Index was also used to evaluate the proportion of premises that were active (moved at least one animal) in two consecutive periods for the hold network, which was divided by the total of premises in both considered times, following equation 3.

$$\text{node loyalty} = \varphi_i^{t-1,t} = \frac{|V^{t-1} \cap V^t|}{|V^{t-1} \cup V^t|} \tag{3}$$

Where V_i^{t-1} is the set of premises that are active in the period $t-1$, and V_i^t is the set of premises that moved at least one animal at time t. For both analysis (loyalty and node-loyalty), we considered a span time t of one year.

The yearly $\varphi_i^{t-1,t}$and $\theta_i^{t-1,t}$are expressed in a value between zero and one, where a $\theta_i^{t-1,t}$ of one indicates that 100% of links with same origin and destination were preserved (100% loyalty between premises); and a value of one in $\varphi_i^{t-1,t}$ means that all premises were active in two consecutive periods, but not is necessarily trading with the same commercial partner.

2.6 Time-windows network analysis

A temporal network was considered, $g = (V, E, T)$, where V is a set of nodes and E a set of edges in each observation period T. Each edge in E is given by a triple (i, j, T) and connects node i and node j at time T. To describe the temporal patterns over time, we used a monthly time-window or series of snapshots, e.g. $g = g_1, \ldots, g_T$. (HOLME; SARAMÄKI, 2012). The descriptive assessment of the temporal network snapshots was made with the same parameters described in the table 2.

2.7 Causal fidelity

Some paths existing between nodes in the static aggregation do not follow a chronological order, and therefore such paths do not exist in the temporal representation. To quantify the quality of a static aggregation, Lentz et al. (2013) defined so-called *causal fidelity,* which measures the proportion of paths in a temporal network which exist in the static counterpart. For this purpose, accessibility matrices are constructed for the static and temporal networks representing the path lengths between each pair of nodes. To calculate the causal fidelity of the network, it is necessary to calculate the *path density* (equation 4), where we defined the density of its accessibility matrix:

$$p(P_n) = \frac{nnz(P_n)}{N^2} \tag{4}$$

where P_n is the accessibility matrix for the path length $n = 0, \ldots, N$, $nnz(P_n)$ is the number of non-zero elements of the accessibility matrix, and N is the number of nodes in the network. In the upper limit of path density, i.e. $p(P_n) = 1$, most nodes can reach each other. On the contrary, for a low path density $p(P_n) = 0$ the network tends to be temporarily disconnected (Lentz et al., 2016)

Causal fidelity is calculated as the quotient of path densities, defined as:

$$\boldsymbol{c} = \frac{p(P_n)}{p(\boldsymbol{\Omega}_n)} = \frac{\text{Number of paths in the temporal network}}{\text{Number of paths in the static network}}. \tag{5}$$

The causal fidelity ranges between $0 \leq c \leq 1$. Large values of c indicate that the static aggregation of a temporal network gives a good approximation from a causal

perspective and low values indicate that the majority of paths in the time-aggregated network are not in the right chronological order (Büttner et al., 2016; Lentz et al., 2016).

2.8 Temporal network vulnerability and resilience

The outgoing contact chain (OCC) quantifies the number of 'downstream' premises that could potentially acquire infection from the *index* premise through outgoing animal movements, adhering to the chronological order of the movements (FIELDING et al., 2019; PAYEN; TABOURIER; LATAPY, 2019).

We use this approach to build the OCC model, which can be viewed as a simplified representation a SI (susceptible- infected) model structure if every between-premise movement results in transmission; a potential outbreak can be seeded at a given time t0 in each node in turn, and the resulting OCC can be considered the outbreak size.

By simulating the OCC across all possible seed nodes, we generated a distribution of the network's OCC sizes. We then calculated the average OCC and 95% CI across all premises using the entire period of study. We quantified the vulnerability of OCCs to the removal of 10, 250, 500, 1000 and 1500 nodes, with the order in which nodes were removed based on network metrics in descending order (Degree, Betweenness, Closeness, PageRank, OCC size), and also selecting Random-nodes. We then analyzed the changes in the mean OCC size over time.

2.9 Network-based risk index

SNA parameters values at the premise-level (Degree, Betweenness, Closeness and the reverse PageRank) were aggregated at the municipality level to visualize spatial hotspots of movement. As a network-based spatial risk index, we re-scaled all network metrics from zero to one, and then summed across all premises to generate the raw risk index and visualized a municipality-level risk map. To calculate the index, we summed the values for a specific SNA parameter (*SNP*) in the municipality as (eq. 6)

$$SNP = \sum \Psi_k \quad (6)$$

Where Ψ is the network parameter (indexed by k premise) in a particular municipality i. The SNP was divided by the maximum value of all SNP within municipalities.

$$index = \frac{SNP_i}{\max(SNP)} \quad (7)$$

Therefore, using equation 7, a network-based risk index of one describes a municipality with the highest risk to receive infected animals by animal movements for the considered network.

Additionally, we also calculated a population-based index that standardized the raw index by the swine population reported for the last year of analysis in each municipality. We scaled the animal population size from zero to one, representing the proportion of animals in the municipality. In order to show the swine population at-risk related to the network-based risk index (equation 7), we scaled the index by swine population, following eq 8,

$$index\ pop = \frac{SNP_i}{\max(SNP)} * \frac{\sum S_k}{\max(\sum S_k)} \quad (8)$$

Where $\sum S_k$ represents the sum of swine population S by premise k in each municipality i. We present the results in two maps, the first showing only the raw index calculation and the second the index scaled by the total of swine population declared for the year 2017.

2.10 Community detection

In the state of SC, epidemiological surveillance and control units are organized at various levels starting at the municipality-level. For that reason, we aggregate the movements made by farms in each municipality, considering the municipality to be a node. This analysis captured spatial connectivity amongst different municipalities via animal movements, including pairs of locations that shared common direct and indirect connections within the network. Community detection was performed using an algorithm based on the calculation of LinkRank, a concept derived from Google's PageRank (BRIN; PAGE, 1998) that takes into account the incoming links of a given municipality and the incoming links of its neighbors (GRISI-FILHO et al., 2013).

We also calculated modularity as a measure of the strength of community structure, where values of 0.3 – 0.7 generally indicate moderate to strong community structure (GRANOVETTER, 1973).

All analysis and data visualization were performed in R statistical software (R CORE TEAM, 2017) version 2.4.2 using the packages: igraph version 1.1.2 (NEPUSZ, 2006),

rgdal version 1.2-8 (KEITT et al., 2018), circlize version 0.4.1 (GU et al., 2014), EpiContactTrace version 0.12.0 (NÖREMARK; WIDGREN, 2014), tidyverse (Hadley Wickham, 2017), sf (PEBESMA, 2018), and the Illustrator CC5 software (GOLDING, 2017). Shapefiles to produce the maps were obtained from the *Instituto Brasileiro de Geografia e Estatística* (www.ibge.gov.br).

3. RESULTS

3.1 Data

The movements included in this study compromised 99.9% of the total available records. A small proportion of records were removed because the number of animals was listed as zero animals or >20000, which were considered errors. In this swine trade network, there were 11,606 premises, and 6,0645,853 pigs involved in 320,814 movements during the period of study.

3.1 Data trade description

Within SC, the dominant trade flow of animals originated from breeding-farms and CSBF and passed through Nurseries to Finisher farms. Finishers received a significant amount of movements from Nursery, Breeding and CSBF premises and, sent the largest flow of movements to Slaughterhouses.

We illustrated the main movements within and between types of premises in Figure 2; for visualization purposes, atypical movements representing less than 1 % of the total of possible connections were excluded (Figure 2). The full description is available in the supplementary table 1.

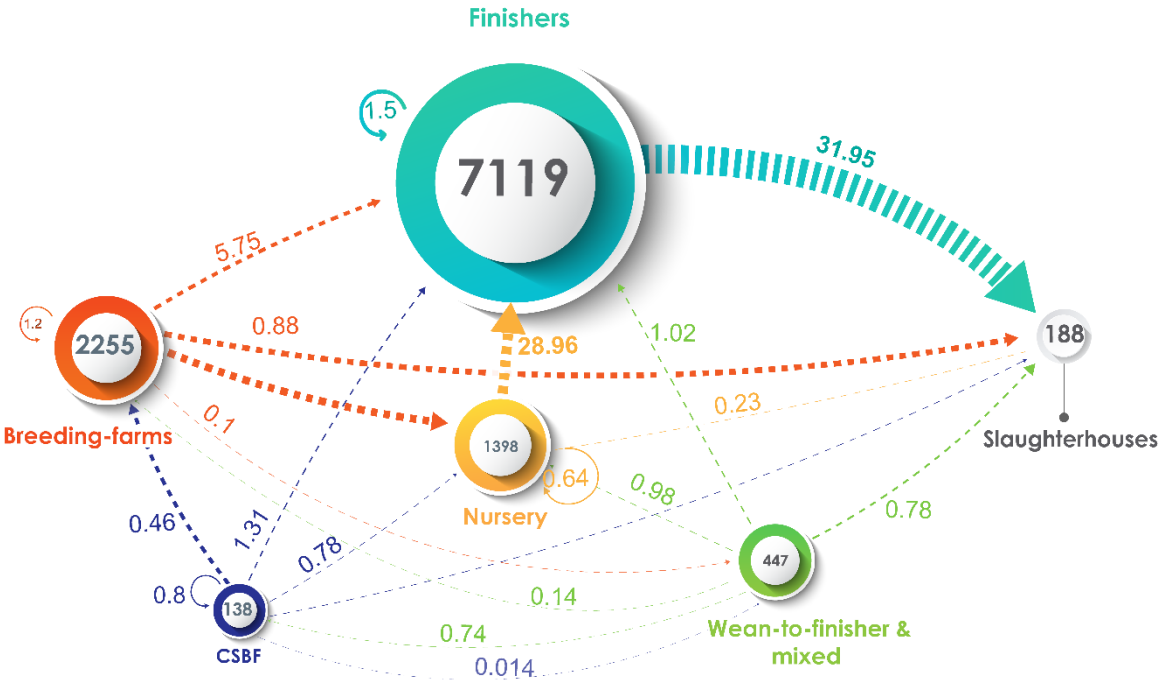

Figure 2. Trade flow in SC state from 2015-01-01 and 2017-12-31. Arrows are weighted by the percentage of total movements and, the color indicates the origin of the movement. Circles represent the total of premises for each type of classification, and the size approximates the total of premises grouped by the circle.

3.2 Static network and Fragmentation

The yearly analysis of the static network showed a slight decrease through time for some metrics (number of nodes and edges, diameter, GSCC, Clustering coefficient and, GWCC) between 2015 and 2016 (Table 3). The GSCC represented just 6.41 % of the total nodes for all years, and we found large differences in the size of the GSCC when we compared the annual networks and the overall network (aggregated across all years). The number of swine moved, graph density, and mean path length increased over time.

The full 2015-17 network had a fragmentation of 0.13 and GWCC of 0.93, whereas the yearly snapshots networks were between 0.06 and 0.09 for fragmentation and 0.95 and 0.96 for the GWCC (Table 3). Taken together, these values indicate that the network exhibits a high degree of connectivity.

Table 3. Description of the annual static network and fragmentation values from 2015 to 2017, and for the overall network (2015-17) in the state of Santa Catarina, Brazil.

The sizes of the components are presented in the number and percentage of total nodes in the network.

Year	Nodes	Edges	Graph Density	GSCC (%)	GWCC (%)	Fragmentation	Total animals moved	Mean Path length	Diameter
2015	9,924	52,091	0.000529	21 (0.21%)	9463 (95%)	0.09	18,955,998	2.90	12
2016	9,598	51,402	0.000559	65 (0.68%)	9191 (95%)	0.08	20,364,474	5.16	17
2017	9,218	46,604	0.000549	22 (0.23%)	8894 (96%)	0.06	21,249,869	5.83	15
ALL YEARS	11,616	112,402	0.000835	744 (6.4%)	10820 (93%)	0.13	60,570,341	7.18	24

At the premises level, in-degree showed a wider distribution than out-degree, with more premises having three to ten unique trading partners (Figure 3a). A visual examination of the distribution of the number of animals moved per premise according to the purpose of the movement showed a correlation between slaughterhouse and reproduction purposes (Figure 3b).

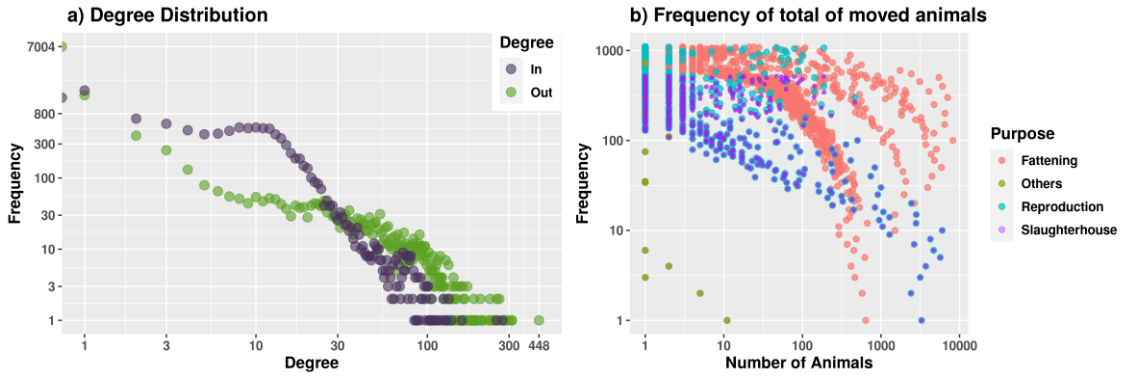

Figure 3. a) Distribution of in- and out-degree for all premises. b) Distribution of the number of animals moved per premises. Both axes are on a base10 logarithmic scale in both panels.

3.3 Edge-loyalty (θ) and node-loyalty (φ) of the network

The union and intersection of the edges and nodes were calculated between consecutive years. Loyalty was far lower from 2016-17 than from 2015-16, even though more than 79% of nodes remained active across the years (Table 4).

Table 4. The proportion of intersection and union and loyalty values from edges and nodes.

Period Of Time	Union Of Edges	Intersection Of Edges	Edge-Loyalty (Θ)	Union Of Nodes	Intersection Of Nodes	Node-Loyalty (φ)
2015-2016	85,833	51,403	0.59	10877	9594	0.88
2016-2017	81,721	16,287	0.19	10487	8319	0.79

3.4 Temporal network

We assessed the temporal network in monthly snapshots, describing the patterns of the pig trade throughout the period of study using the parameters described in table 2. The number of nodes and edges decreased over time, ranging between 3548 to 4157 and 7849 to 9979, respectively. The mean and sum of pigs moved per movement increased over time. The percentage of the GSCC and GWCC varied through time without an apparent temporal trend. Graph density, clustering coefficient, and in-degree centralization showed a peak value in the middle of the year 2016 (figure 4).

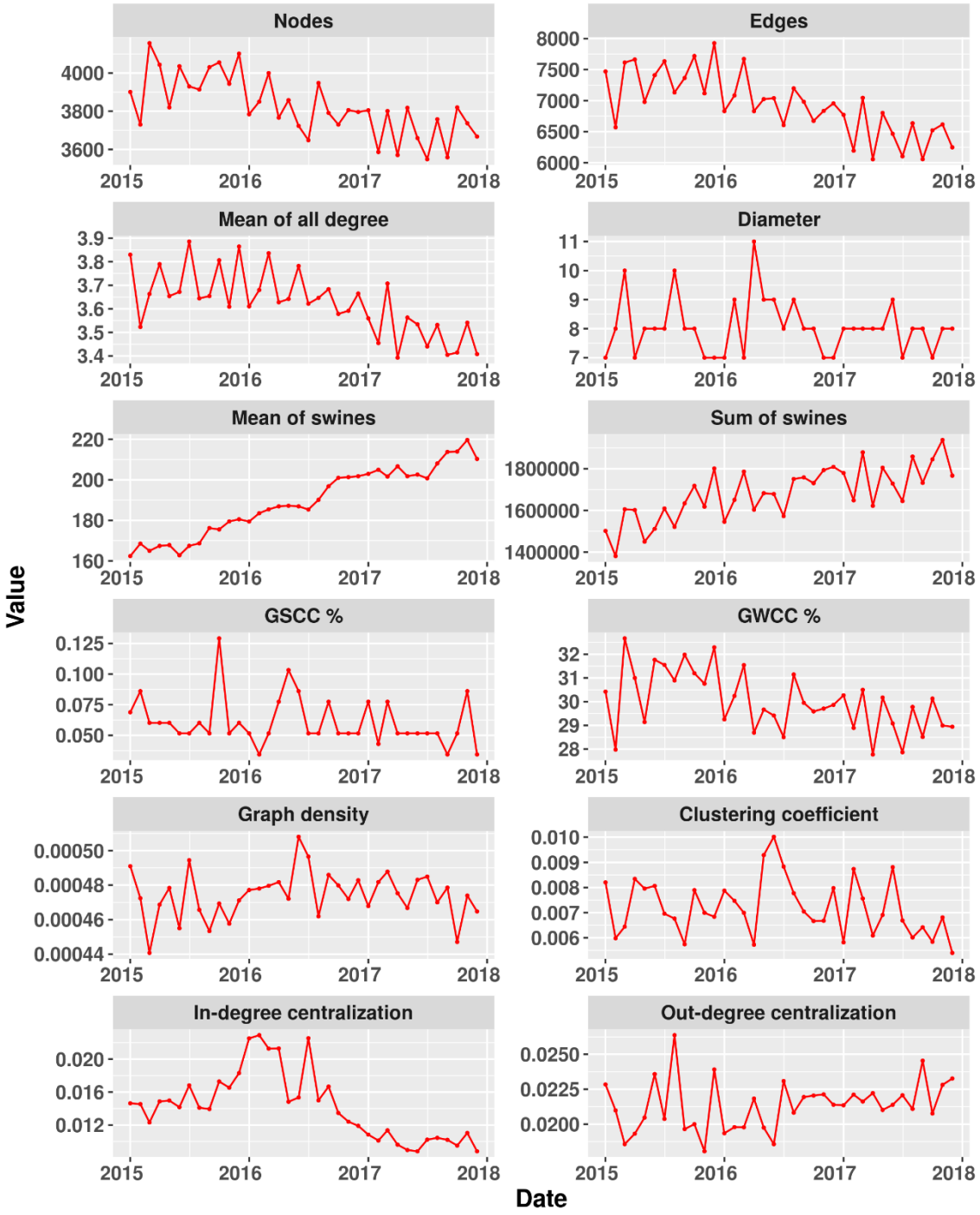

Figure 4. Description of the temporal network using a monthly time- snapshots network by network-level metrics; more details about the metrics are shown in supplementary table 1.

3.5 Causal fidelity

For the whole observation period, 11,226,066 paths were observed in the static network but only 1,287,009 time-respecting paths in the temporal network could be obtained, which results in a causal fidelity of 0.11. Thus, about 11% of the time-respecting paths exist in both network representations, indicating that the static representation of the network poorly captured the features of the temporal network.

3.6 Temporal network vulnerability and resilience

The size of the OCC (outgoing contact chain) was calculated for all nodes. In general, the removal of nodes based on degree, betweenness, and reverse PageRank resulted in greater decreases in the OCC sizes as compared to the removal of nodes based on PageRank or at random (Figure 5). The removal of only 10 nodes had a little impact regardless of how the removed nodes were selected. However, targeted removal of >250 highly connected nodes resulted in a noticeable decrease in OCC. Removal of just 250 nodes (2.15% of the total network) led to up to a 50% decrease in mean OCC when using degree as the targeting metric. The complete distribution values for each SNA parameter after each node removal were plotted (supplementary figure 1), and for visualization, the mean and confidence intervals are shown by week (Figure 5).

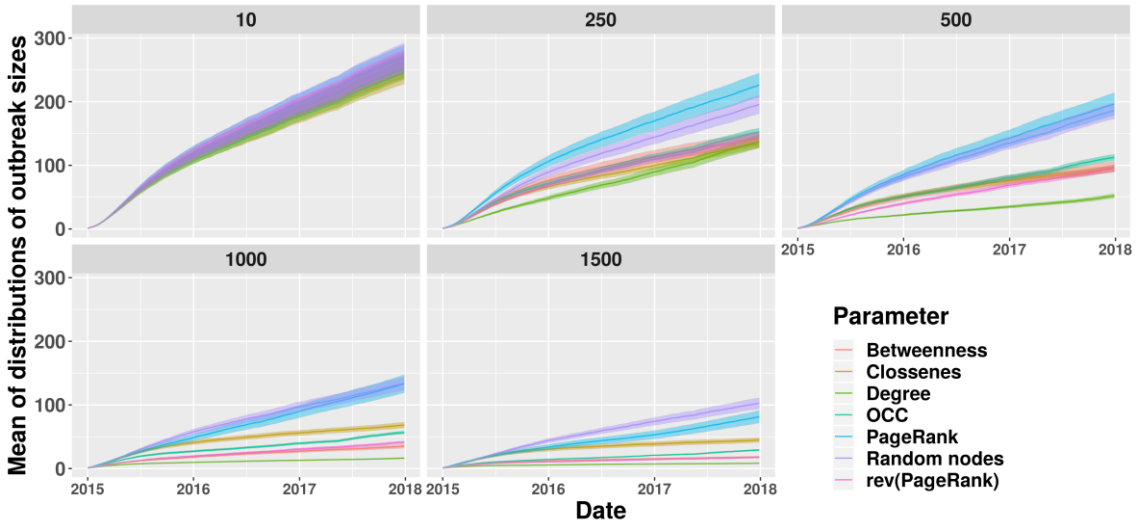

Figure 5. Temporal network vulnerability. Each line represents the average of the size of the outgoing contact chain (OCC) through time after removal of the top 10, 250, 500, 750 and 1000 nodes ranked according to various network parameters. The colored shaded areas represent confidence interval (CI 95%).

Figure 6 shows the frequencies of OCCs resulting from the removal of 10 – 1500 nodes. When 1500 nodes were removed, selection of nodes based on d*egree* resulted in a lower OCC sizes distribution, followed by reverse PageRank and betweenness.

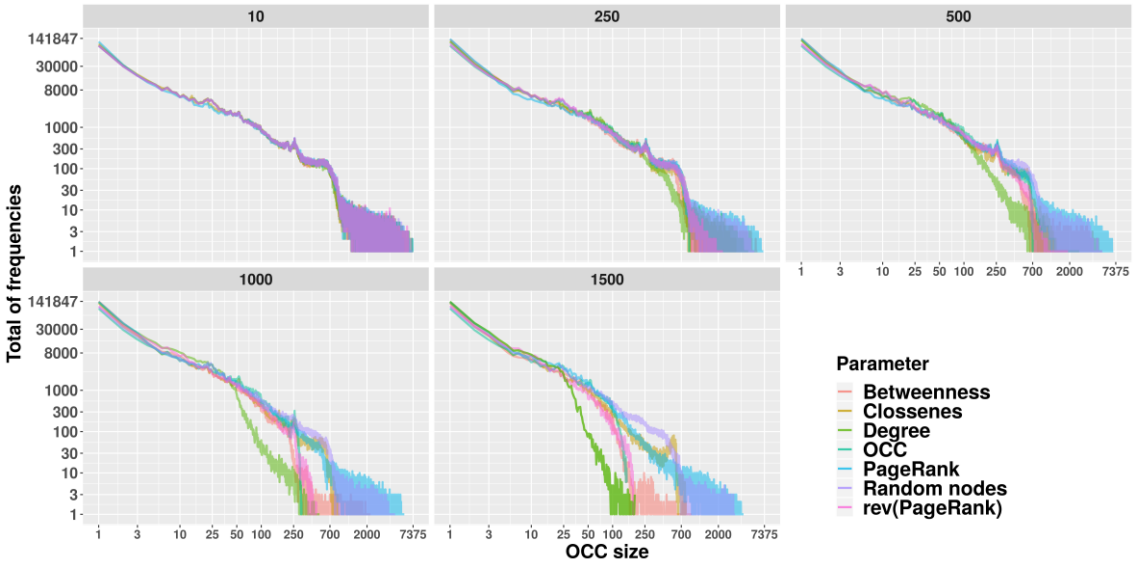

Figure 6. Mined data of frequencies of OCCs resulting from the node after removal of the top 10, 250, 500, 750 and 1000 nodes ranked according to various network parameters. Each line color represents a SNA parameter.

3.7 Network-based risk index

From the above analysis, we can discriminate the parameters that best capture the temporal network's vulnerability and resilience. Thus, we selected the parameters that resulted in the greatest reduction in OCC (Degree, Betweenness, Closeness, and reverse PageRank) for our network-based risk $index$ **and** $index\ pop$. These indexes were calculated to quantify spatial patterns and identify municipalities that were hotspots for movement. The network-based results, either raw or standardized for swine population size, are shown in Figures 7 and 8, respectively. The municipalities that played a key role in the pig trade network in SC state for both maps were Concórdia, Seara, and Videira.

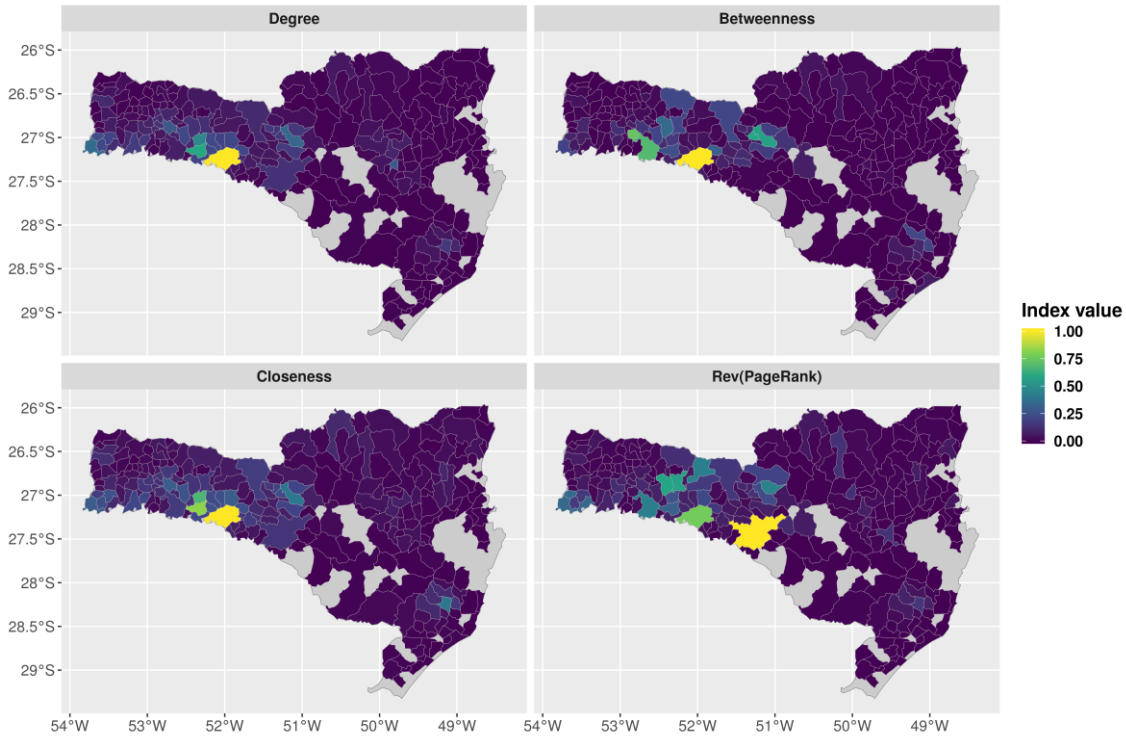

Figure 7. Map of the network-based risk *index* by municipality from SC State, Brazil. The maps are faceted by SNA parameter (Degree, Betweenness, Closeness and finally Rev(PageRank)).

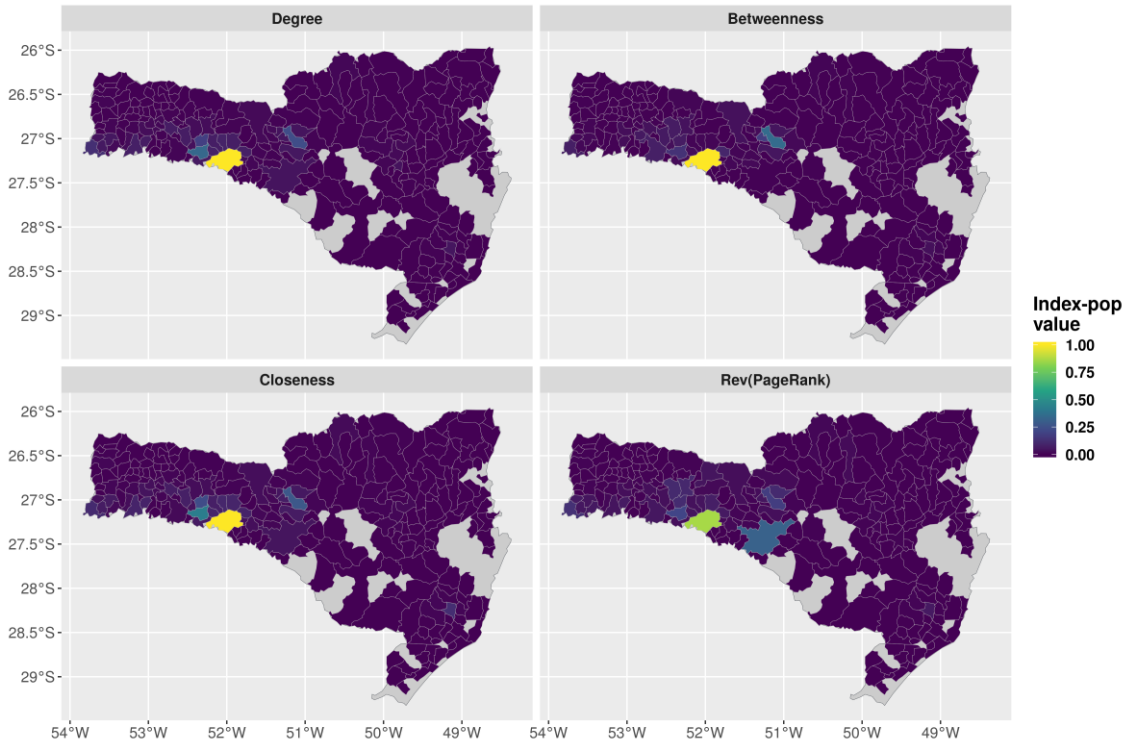

Figure 8. Map of the Network-based risk $index\ pop$ here was considered the swine population in each municipality from SC, Brazil. The maps are faceted by SNA parameter (Degree, Betweenness, Closeness and finally Rev(PageRank)).

3.8 Communities

Communities are sets of nodes (municipalities in this case) that interact more frequently with one another than with nodes from other communities. The spatial distribution and the proportion of the movements within communities are shown in figure 9. The modularity value was 0.35, indicating a moderate community division. As shown in figure 1, there are no premises located in certain municipalities and therefore they could not be assigned to a specific community (NA in figure 9b).

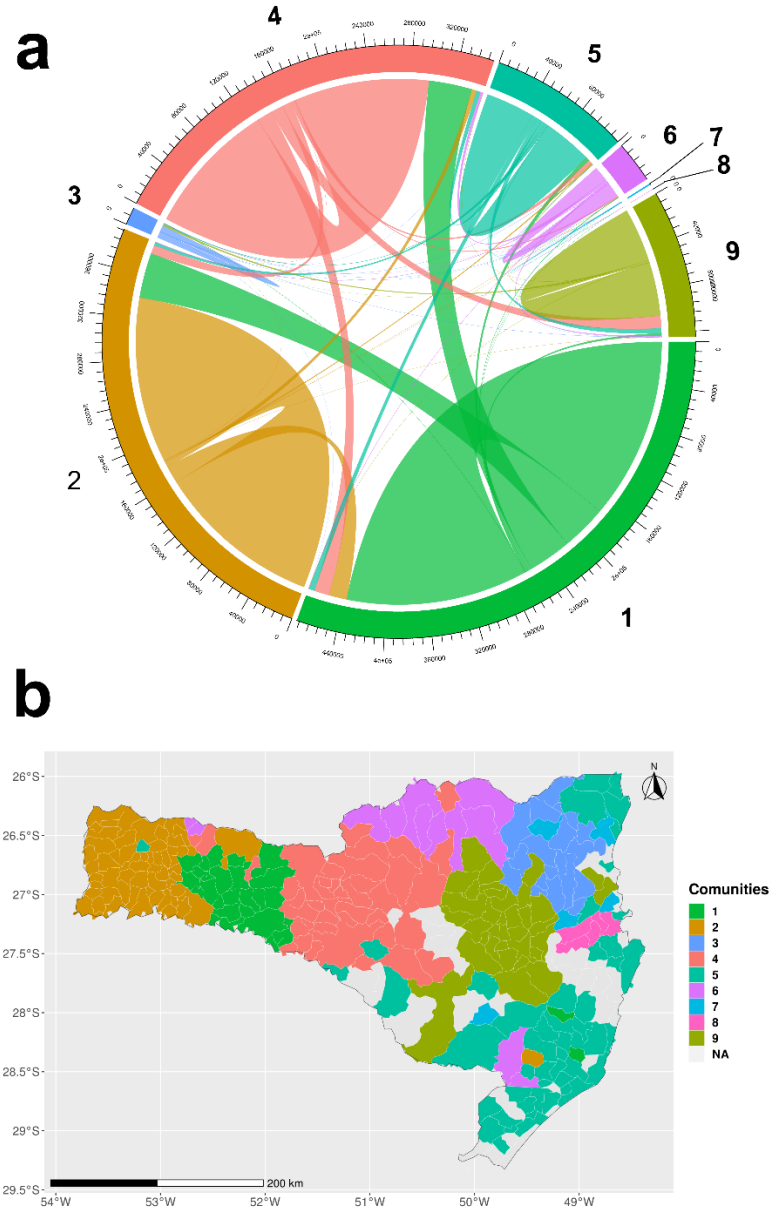

Figure 9. Spatial and structural characterization of the largest trade communities. Color indicates the community membership. a) Circular plot for intra- and inter-community movement flows. Each sector of the circle represents a community. The

outgoing animal flow starts from the base of each sector. (b) Map of the state of Santa Catarina, Brazil with the geographical locations of the communities by the municipality. NA represents municipalities without reported movements.

4 DISCUSSION

In this research, we use a two-pronged approach (static and temporal) network analysis aimed at exploring and characterizing pig trade at global and node levels in Santa Catarina, Brazil. We also propose a methodology for ranking high-risk areas for enhancing control and surveillance in communicable diseases considering the dynamics of swine trade. We used a static network analysis approach to describe the general structure of the network (Table 3 and Fig. 2) and temporal analysis to describe the dynamic trends using monthly snapshots (Fig. 4). Since we found a low value of causal fidelity, we used the OCC approach that considers time-respecting paths to analyze the vulnerability of the network to targeted node removal (Fig. 5 and Fig 6.). To understand the spatial distribution of risk, we calculated a risk index to prioritize the control and surveillance actions at the municipality level (Fig. 7 and Fig. 8) and performed a community analysis to describe the flux of movements between municipalities (Fig. 9).

In the static network analysis, the results of our loyalty analysis (nodes and edges) suggest that the commercial relationships from one year to another were not highly conserved despite the fact that a large portion of the nodes were active in both periods of time. There was also a drastic decrease in edge loyalty from 0.59 to 0.19 across the two periods observed. In addition, the proportion of nodes that remained active from year-to-year fell from 0.88 to 0.79. These patterns could exacerbate the potential for the spread of infectious diseases because many connections over time are not predictable.

The observed degree distributions showed scale-free properties, with many premises trading animals with only a few direct partners and a small number of premises trading with many direct partners. Above a value of 30, high out-degree premises were more common than high in-degree premises (Fig. 3). This is mainly given by the degree distribution of Breeding-farms and Nursery-farms (supplementary Fig. 2), reflecting vertical integration of production chains. The pyramidal structure of the production chain also may explain the low sizes of GSCCs, whereas GWCCs

showed high levels of connectivity, compromising more than 95% of the network (table 4).

In the analysis of temporal trends, we found a decreasing number of active nodes and edges but an increasing number of swine moving throughout the study (Fig. 4). These findings suggest an increase in the size of premises and number of animals mobilized. Similar trends also were observed in Swedish and Danish pig trade (NÖREMARK et al., 2011; SCHULZ et al., 2017; STERCHI et al., 2019). Moreover, monthly values for the clustering coefficient and graph density were similar to mid-range values reported in other livestock networks (NÖREMARK et al., 2011; MWEU et al., 2013; VANDERWAAL et al., 2016b; FIELDING et al., 2019). We could not detect clear seasonal activity patterns as observed in others pig trade networks (KONSCHAKE et al., 2013; BÜTTNER; SALAU; KRIETER, 2016).

Given that static networks are more straight-forward to analyze, it is essential to understand the fidelity of the static network in representing a temporally dynamic network. To answer this, we followed the methodology proposed by Lentz et al., and demonstrated a low causal fidelity value. This indicates that the static networks may lead to an over-representation of the true connectivity of the network (LENTZ; SELHORST; SOKOLOV, 2013; LEBL et al., 2016), and thus inappropriate assessments of risk or design of control strategies. If the disease dynamics are slow in relation to the dynamics of the network, the results of the static network analysis may be sufficient to explain and predict a possible disease transmission (HOLME; SARAMÄKI, 2012). However, the use of a static representation for disease models may systematically overestimate the results of outbreak size, particularly for rapidly spreading diseases (LENTZ; SELHORST; SOKOLOV, 2013; KNIFIC et al., 2020).

Therefore, the use of temporal OCC analyses provides a better approach to evaluate the impact of target control because it incorporates the chronological nature of animal movements. The literature on temporal network analysis uses many terms to describe the OCC concept, such as time-directed paths, source counts, accessible worlds, output domains, reachability, unfolding accessibility, and recently spreading cascades (PAYEN; TABOURIER; LATAPY, 2019; KNIFIC et al., 2020). All of these terms describe a temporally sequential network to identify the nodes that are accessible through edges to/from each index node within a selected time period

(FIELDING et al., 2019). We selected the term OCC to describe the number of nodes that could be reached from a certain premise, and this process represents a simple Susceptible-Infected (SI) model assuming a 100% infection rate via animal movements using the time-respecting paths. Thus, testing targeted control actions under this scenario provides useful information for field performance (VIDONDO; VOELKL, 2018; PAYEN; TABOURIER; LATAPY, 2019).

The most common strategies to contain an epidemic outbreak include culling, isolation of holdings, increased hygiene measures, and vaccination, among others (MOTTA et al., 2017). Targeting these measures towards premises with high centrality can be an effective strategy for efficient disease control. Analysis of the impact of targeted node removal on network connectivity generally measure the impact of removals on the size of the GWCC and GSCC (BÜTTNER et al., 2013; LENTZ et al., 2016; MARQUETOUX et al., 2016; MOTTA et al., 2017; CHATERS et al., 2019), which does not account for temporal dynamics. For this reason, we used reductions in the mean size of OCC to measure the efficacy of targeted removals, thus accounting for time-respecting paths.

Based on this analysis, we showed that prioritizing the removal of farms based on degree substantially reduced the potential for transmission of an infectious pathogen in the contact network as compared to removing farms at random. Therefore, control actions should be focused on high degree farms, such as Nursery and Breeding-farms (see supplementary Fig 2). In our study, a >90% decrease in the mean OCC mean was achieved by removing just 1000 nodes, which is particularly important in surveillance and control systems with limited resources.

We proposed a network-based index classification to target surveillance actions and assist surveillance authorities to classify areas (municipalities) according to the probability and consequence of certain areas becoming infected via in/out movements. The selection of the metrics to compose the indexes was based on the network metrics that were most effective at reducing the size of the OCC (Degree, Betweenness, Closeness) and the reverse of PageRank). Hence, we identified nodes at the beginning of the contact chain that traded with hubs of the network that, in theory, might be the beginning of the production chain and therefore have an important role in the disease spreading. Based on these, we implemented the Reverse of PageRank as network

metric, due these nodes that can induce bigger changes in the mean OCC after node removal.

We also standardized these *indexes* according to the swine population of each region, thus creating a visualization of the most important regions which could be prioritized for control actions. These geographical areas were highly correlated with farm density (Figs. 1 and 8), which was one of the motivations to carry out the community analysis.

We found 9 large trade communities in SC State. Communities 1, 2 and 4 were geographically connected and registered the 60.8% of animal movements. Inter-community trade flux represented just 23.6% of movements, and most main flows were from community 1 to communities 2 and 4 (11.1%). The main purposes for the latter were slaughter (8.17%), fattening (2.28%) and reproduction (0.64%), thus the southwest region of SC state is the most important for swine trade based on both high internal trade and density of premises (See figure 1 and 9). The use of communities offers the opportunity to control outbreaks through zonation or compartmentalization by sub-dividing the state into sectors in which movements are more frequent within sectors than between sectors (OIE, 2019). Thus, if one sector were to become infected, trade in other sectors could potentially be protected via coordination of inter- and intra-sector disease management strategies (CHRISTLEY et al., 2005; LENTZ et al., 2011; GRISI-FILHO et al., 2013; GORSICH et al., 2016).

Animal movements are just one aspect of the epidemiology of infectious diseases. Despite the importance of movements (O'HARA et al., 2020; VANDERWAAL et al., 2020) network analysis should be undertaken in conjunction with other epidemiological tools. Several limitations of our work include that we were not able to include the effects of illegal movements and their influence on the network. We also could not rule out the possibility that an animal diseases outbreak could affect the dynamics of the network. This study also assumes that transmission of diseases related to the outgoing contact chain spread only via animal movements and that each movement is successful in disease transmission, which likely results in an overestimate of OCC size. Furthermore, we inherently neglected other potential transmission pathways such as movement of other susceptible or non-susceptible animal species, movement of owners, workers or veterinarians, transmission via vehicles, shared equipment or bioaerosols (KNIFIC et al., 2020), etc., which may have

resulted in an under-approximation of the worst-case scenario for the introduction and spread of an exotic animal disease.

5 CONCLUSION

The network analysis and indexes presented here provide useful data to rank premises and guide the development of targeted surveillance and control schemes. We documented temporal and spatial patterns of trade, and outline how this temporal and spatial variation could be used to design data-informed strategies for disease surveillance and control.

6 REFERENCES

BAJARDI, P. et al. Optimizing surveillance for livestock disease spreading through animal movements. **Journal of The Royal Society Interface**, v. 9, n. 76, p. 2814–2825, nov. 2012.

BORGATTI, S. P. Identifying sets of key players in a social network. **Computational and Mathematical Organization Theory**, v. 12, n. 1, p. 21–34, abr. 2006.

BRIN, S.; PAGE, L. The anatomy of a large-scale hypertextual Web search engine. **Computer Networks and ISDN Systems**, v. 30, n. 1–7, p. 107–117, abr. 1998.

BÜTTNER, K. et al. Efficient Interruption of Infection Chains by Targeted Removal of Central Holdings in an Animal Trade Network. **PLoS ONE**, v. 8, n. 9, p. e74292, 2013.

BÜTTNER, K.; SALAU, J.; KRIETER, J. Quality assessment of static aggregation compared to the temporal approach based on a pig trade network in Northern Germany. **Preventive Veterinary Medicine**, v. 129, p. 1–8, jul. 2016.

CHATERS, G. L. et al. Analysing livestock network data for infectious disease control: an argument for routine data collection in emerging economies. **Philosophical Transactions of the Royal Society B: Biological Sciences**, v. 374, n. 1776, p. 20180264, jul. 2019.

CHRISTLEY, R. M. et al. Infection in Social Networks: Using Network Analysis to Identify High-Risk Individuals. **American Journal of Epidemiology**, v. 162, n. 10, p. 1024–1031, nov. 2005.

EMBRAPA. **Empresa Brasileira de Pesquisa Agropecuária**.

FIELDING, H. R. et al. Contact chains of cattle farms in Great Britain. **Royal Society Open Science**, v. 6, n. 2, p. 180719, fev. 2019.

FREEMAN, L. C. Centrality in social networks conceptual clarification. **Social Networks**, v. 1, n. 3, p. 215–239, jan. 1978.

GOLDING, with M. **Adobe Illustrator CS5 : for web and interactive design**Ventura, CA : Lynda.com, [2010] ©2010, , 2017. .

GORSICH, E. E. et al. Mapping U.S. cattle shipment networks: Spatial and temporal patterns of trade communities from 2009 to 2011. **Preventive Veterinary Medicine**, v. 134, n. Supplement C, p. 82–91, nov. 2016.

GRANOVETTER, M. S. The Strength of Weak Ties. **American Journal of Sociology**, v. 78, n. 6, p. 1360–1380, 1973.

GRISI-FILHO, J. H. H. et al. Detecting livestock production zones. **Preventive Veterinary Medicine**, v. 110, n. 3–4, p. 304–311, jul. 2013.

GU, Z. et al. circlize implements and enhances circular visualization in R. **Bioinformatics**, v. 30, n. 19, p. 2811–2812, out. 2014.

HOLME, P.; SARAMÄKI, J. Temporal networks. **Physics Reports**, v. 519, n. 3, p. 97–125, out. 2012.

KEITT, T. et al. **rgdal: Bindings for the Geospatial Data Abstraction Library**, jan. 2018. .

KNIFIC, T. et al. **Implications of Cattle Trade for the Spread and Control of Infectious Diseases in Slovenia Frontiers in Veterinary Science** , 2020. .

KONSCHAKE, M. et al. On the Robustness of In- and Out-Components in a Temporal Network. **PLoS ONE**, v. 8, n. 2, p. e55223, fev. 2013.

LEBL, K. et al. Impact of Network Activity on the Spread of Infectious Diseases through the German Pig Trade Network. **Frontiers in Veterinary Science**, v. 3, n. June, p. 48, 2016.

LENTZ, H. H. K. et al. Trade communities and their spatial patterns in the German pork production network. **Preventive Veterinary Medicine**, v. 98, n. 2–3, p. 176–181, fev. 2011.

LENTZ, H. H. K. et al. Disease Spread through Animal Movements: A Static and Temporal Network Analysis of Pig Trade in Germany. **PLoS ONE**, v. 11, n. 5, p. e0155196, maio 2016.

LENTZ, H. H. K.; SELHORST, T.; SOKOLOV, I. M. Unfolding Accessibility Provides a Macroscopic Approach to Temporal Networks. **Physical Review Letters**, v. 110, n. 11, p. 118701, mar. 2013.

MAPA. **Caracterização dos sistemas produtivos brasileiros**.

MARQUETOUX, N. et al. Using social network analysis to inform disease control interventions. **Preventive Veterinary Medicine**, v. 126, p. 94–104, abr. 2016.

MOSLONKA-LEFEBVRE, M. et al. Market analyses of livestock trade networks to inform the prevention of joint economic and epidemiological risks. **Journal of the Royal Society Interface**, v. 13, n. 116, p. 20151099, mar. 2016.

MOTTA, P. et al. Implications of the cattle trade network in Cameroon for regional disease prevention and control. **Scientific Reports**, v. 7, n. 1, p. 43932, dez. 2017.

MWEU, M. M. et al. Temporal characterisation of the network of Danish cattle movements and its implication for disease control: 2000–2009. **Preventive Veterinary Medicine**, v. 110, n. 3–4, p. 379–387, jul. 2013.

NEPUSZ, G. C. and T. The igraph software package for complex network research. **InterJournal**, v. Complex Sy, p. 1695, 2006.

NÖREMARK, M. et al. Network analysis of cattle and pig movements in Sweden: Measures relevant for disease control and risk based surveillance. **Preventive Veterinary Medicine**, v. 99, n. 2, p. 78–90, 2011.

NÖREMARK, M.; WIDGREN, S. EpiContactTrace: an R-package for contact tracing during livestock disease outbreaks and for risk-based surveillance. **BMC Veterinary Research**, v. 10, n. 1, p. 71, 2014.

O'HARA, K. et al. Network Analysis of Swine Shipments in China: The First Step to Inform Disease Surveillance and Risk Mitigation Strategies. **Frontiers in Veterinary Science**, v. 7, p. 189, 28 abr. 2020. Disponível em: <https://pubmed.ncbi.nlm.nih.gov/32411733>.

OIE. **Terrestrial Animal Health Code**. Disponível em: <https://www.oie.int/fileadmin/home/eng/health_standards/tahc/current/chapitre_zoning_compartment.pdf >. Acesso em: 29 jul. 2020.

PAYEN, A.; TABOURIER, L.; LATAPY, M. Spreading dynamics in a cattle trade network: Size, speed, typical profile and consequences on epidemic control strategies. **PLOS ONE**, v. 14, n. 6, p. e0217972, jun. 2019.

PEBESMA, E. Simple Features for R: Standardized Support for Spatial Vector Data. **The R Journal**, v. 10, n. 1, p. 439, 2018.

R CORE TEAM. **R: A language and environment for statistical computing**Vienna, Austria, AustriaR fundation for Statistical Computing, , 2017. .

SCHULZ, J. et al. Network analysis of pig movements: Loyalty patterns and contact chains of different holding types in Denmark. **PLOS ONE**, v. 12, n. 6, p. e0179915, jun.

2017.

STERCHI, M. et al. The pig transport network in Switzerland: Structure, patterns, and implications for the transmission of infectious diseases between animal holdings. **PLOS ONE**, v. 14, n. 5, p. e0217974, maio 2019.

VALDANO, E. et al. Predicting Epidemic Risk from Past Temporal Contact Data. **PLOS Computational Biology**, v. 11, n. 3, p. e1004152, mar. 2015.

VANDERWAAL, K. et al. Evaluating empirical contact networks as potential transmission pathways for infectious diseases. **Journal of The Royal Society Interface**, v. 13, n. 121, p. 20160166, ago. 2016a.

VANDERWAAL, K. et al. Contrasting animal movement and spatial connectivity networks in shaping transmission pathways of a genetically diverse virus. **Preventive Veterinary Medicine**, v. 178, p. 104977, maio 2020. Disponível em: <http://www.sciencedirect.com/science/article/pii/S0167587719309079>.

VANDERWAAL, K. L. et al. Network analysis of cattle movements in Uruguay: Quantifying heterogeneity for risk-based disease surveillance and control. **Preventive Veterinary Medicine**, v. 123, p. 12–22, jan. 2016b.

VIDONDO, B.; VOELKL, B. Dynamic network measures reveal the impact of cattle markets and alpine summering on the risk of epidemic outbreaks in the Swiss cattle population. **BMC Veterinary Research**, v. 14, n. 1, p. 88, dez. 2018.

WASSERMAN, S.; FAUST, K. **Social Network Analysis: Methods and Applications**. [s.l.] Cambridge University Press, 1994.

WATTS, D. J.; STROGATZ, S. H. Collective dynamics of ‘small-world’ networks. **Nature**, v. 393, n. 6684, p. 440–442, jun. 1998.

7 SUPPLEMENTARY MATERIAL

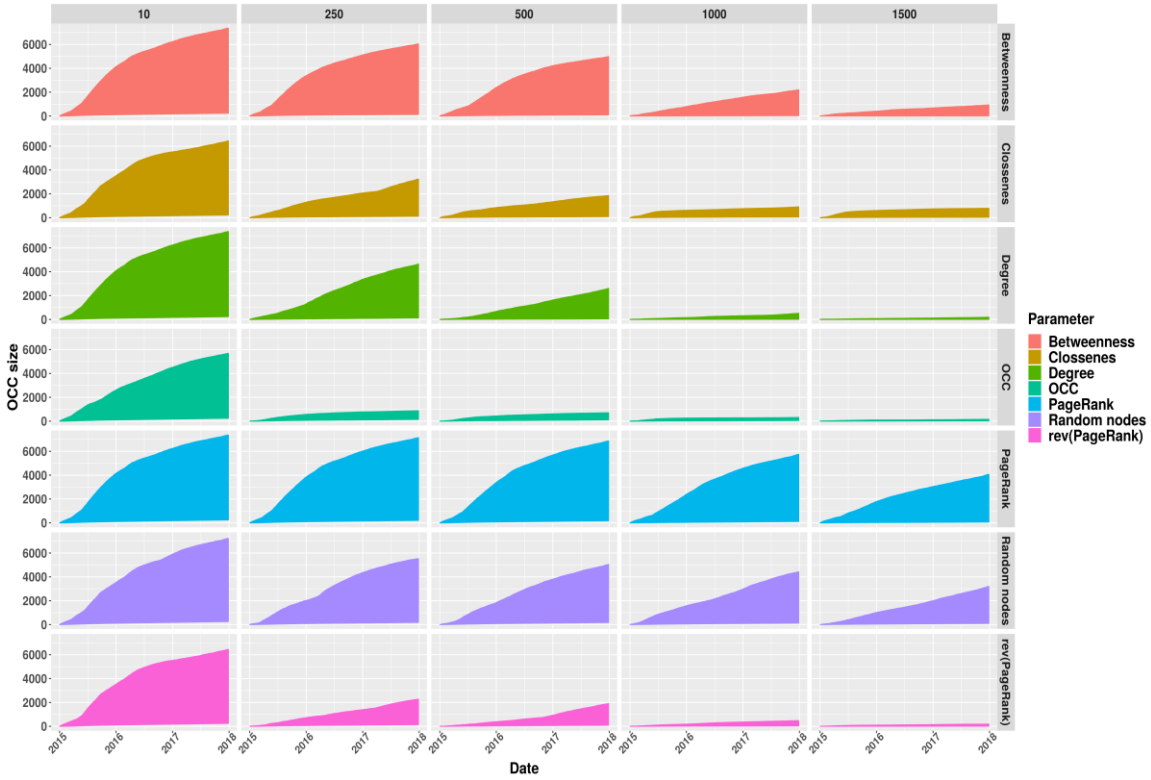

Supplementary Figure 1. Each line represents the average of the outgoing contact chain after remove 10, 250, 500, 750 and 1000 nodes ranked by the higher values network parameter. The colored shaded areas of the lines represent the maximum and minimum values over all study period.

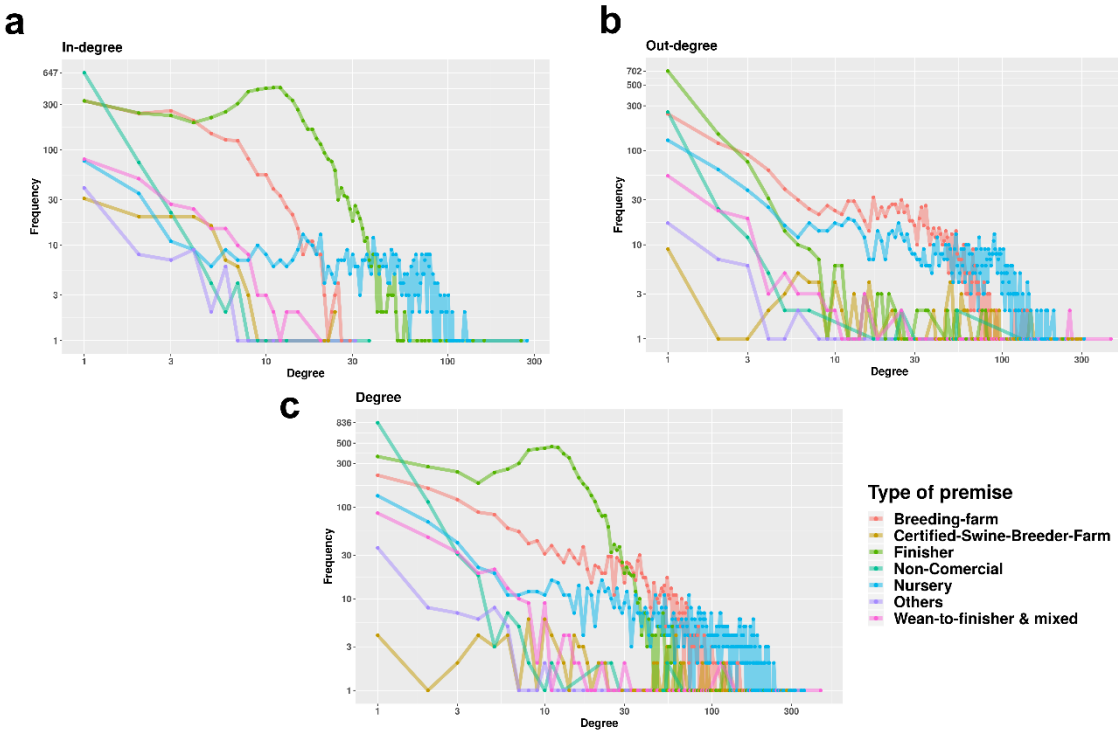

Supplementary Figure 2. Degree distribution by type of premises in SC, stated from 2015-2018. The space breaks between the numbers in the x and y axis are on a base10 logarithmic scale. a) In-degree degree distribution of premises, b) out-degree distribution of premises, c) Degree or all degree distribution of the premises.

Supplementary table 1. Number and proportion of animals and movements within types of premises in SC state from 2015 to 2017

Origin	Destination	movements	Animals	mov. percentage	Ani. percentage
Finisher	Slaughterhouse	332446	29596902	43,97	31,951
Nursery	Finisher	116052	26831783	15,349	28,966
Breeding-farm	Nursery	77192	19619039	10,21	21,179
Breeding-farm	Slaughterhouse	64277	815985	8,501	0,881
Certified-Swine-Breeder-Farm	Breeding-farm	35391	430150	4,681	0,464
Breeding-farm	Finisher	28357	5327584	3,751	5,751
Wean-to-finisher & mixed	Slaughterhouse	16897	726551	2,235	0,784
Wean-to-finisher & mixed	Breeding-farm	13241	137096	1,751	0,148
Certified-Swine-Breeder-Farm	Slaughterhouse	10780	565621	1,426	0,611
Finisher	Finisher	8184	1410404	1,082	1,523
Certified-Swine-Breeder-Farm	Certified-Swine-Breeder-Farm	6078	1139240	0,804	1,23
Nursery	Slaughterhouse	5990	214461	0,792	0,232
Nursery	Nursery	5957	597774	0,788	0,645

Certified-Swine-Breeder-Farm	Finisher	5436	1217011	0,719	1,314
Wean-to-finisher & mixed	Finisher	5122	945689	0,677	1,021
Non-Comercial	Slaughterhouse	4281	49196	0,566	0,053
Finisher	Breeding-farm	2668	37294	0,353	0,04
Certified-Swine-Breeder-Farm	Nursery	2498	730581	0,33	0,789
Wean-to-finisher & mixed	Nursery	2326	913646	0,308	0,986
Wean-to-finisher & mixed	Certified-Swine-Breeder-Farm	1821	693303	0,241	0,748
Others	Breeding-farm	1681	13438	0,222	0,015
Certified-Swine-Breeder-Farm	Wean-to-finisher & mixed	1238	32737	0,164	0,035
Wean-to-finisher & mixed	Wean-to-finisher & mixed	823	51564	0,109	0,056
Breeding-farm	Wean-to-finisher & mixed	792	120578	0,105	0,13
Finisher	Nursery	558	61907	0,074	0,067
Others	Slaughterhouse	558	18618	0,074	0,02
Non-Comercial	Non-Comercial	481	2658	0,064	0,003
Breeding-farm	Breeding-farm	457	7913	0,06	0,009
Non-Comercial	Breeding-farm	423	5277	0,056	0,006
Nursery	Non-Comercial	416	23460	0,055	0,025
Non-Comercial	Finisher	371	58790	0,049	0,063
Breeding-farm	Certified-Swine-Breeder-Farm	310	77071	0,041	0,083
Others	Wean-to-finisher & mixed	292	5345	0,039	0,006
Non-Comercial	Nursery	271	21080	0,036	0,023
Breeding-farm	Non-Comercial	267	21617	0,035	0,023
Wean-to-finisher & mixed	Non-Comercial	263	5962	0,035	0,006
Finisher	Certified-Swine-Breeder-Farm	249	6567	0,033	0,007
Others	Certified-Swine-Breeder-Farm	218	4246	0,029	0,005
Finisher	Non-Comercial	194	4717	0,026	0,005
Finisher	Wean-to-finisher & mixed	161	6071	0,021	0,007
Nursery	Wean-to-finisher & mixed	155	27453	0,021	0,03
Certified-Swine-Breeder-Farm	Others	144	10512	0,019	0,011
Breeding-farm	Others	134	16330	0,018	0,018
Wean-to-finisher & mixed	Others	63	2801	0,008	0,003
Finisher	Others	57	2134	0,008	0,002
Certified-Swine-Breeder-Farm	Non-Comercial	52	629	0,007	0,001
Nursery	Others	51	11436	0,007	0,012
Others	Finisher	39	2512	0,005	0,003
Nursery	Certified-Swine-Breeder-Farm	23	7760	0,003	0,008
Non-Comercial	Wean-to-finisher & mixed	22	223	0,003	0
Others	Non-Comercial	11	33	0,001	0
Others	Nursery	8	88	0,001	0
Others	Others	7	151	0,001	0
Non-Comercial	Others	1	2	0	0

CHAPTER 2

NETWORK ANALYSIS AND TEMPORAL DISEASE SPREAD MODEL TO TARGETED CONTROL ACTIONS FOR BOVINE TUBERCULOSIS IN A STATE FROM BRAZIL

Abstract

Livestock movements create complex dynamic interactions among premises that can be represented, interpreted, and used for epidemiological purposes. These movements are a very important part of the production chain but may also contribute to the spread of infectious diseases through the transfer of infected animals over large distances Social network analysis (SNA) can be used to characterize cattle trade patterns and to identify highly connected premises that may act as hubs in the movement network, which could be subjected to targeted control measures in order to reduce the transmission of communicable diseases such as bovine tuberculosis (TB). Here, we analyzed data on cattle movement and slaughterhouse surveillance for detection of TB-like lesions (TLL) over the 2016-2018 period in the state of Rio Grande do Sul (RS) in Brazil with the following aims: i) to characterize cattle trade describing the static full, yearly, and monthly snapshots of the network contact trade, ii) to identify clusters of premises from which animals with TLL in the space and contact networks, and iii) to evaluate the potential of targeted control actions to decrease TB spread in the cattle population of RS using a stochastic metapopulation disease transmission model that simulated within-farm and between-farm disease spread. We found heterogeneous densities of premises and animals in the study area; the analysis of the contact network revealed a highly connected trade > 94%, with strong temporal trends especially for May and November; the TLL cases were significantly clustered in space, and the contact network, suggesting the potential for both fence-to-fence and movement-mediated TB transmission. According to the disease spread model, removing the 7% highest connected farms based on degree and betweenness could reduce the total number of infected farms over three years by >50%. In conclusion, the characterization of the cattle network suggests that highly connected farms may play a role in TB dissemination, although being close to infected farms was also identified as a risk factor of having animals with TLL. Surveillance and control actions based on degree and betweenness could be useful to break the transmission cycle between premises in RS.

1. INTRODUCTION

Livestock movements create complex dynamic interactions among premises that can be represented, interpreted, and used for epidemiological purposes (BAJARDI et al., 2011, 2012; MOSLONKA-LEFEBVRE et al., 2016). These movements are a very important part of the production chain but may also contribute to the spread of infectious diseases through the transfers of infected animals within premises over large distances (ORTIZ-PELAEZ et al., 2006; PAYEN; TABOURIER; LATAPY, 2019).

Movements between premises are not distributed homogeneously. Instead, some premises usually play a key role in the trade flow and could therefore have a higher risk of being exposed to infectious diseases and of contributing to their spread (GILBERT et al., 2005; ORTIZ-PELAEZ et al., 2006). For this reason, the identification of these premises can be a very useful tool for disease control and eradication programs in order to help minimizing disease transmission. One of the diseases target of control programs in many countries around the world is bovine tuberculosis (TB), and specifically in Brazil is the focus of the National Control and Eradication Program of Bovine Tuberculosis (LAGE et al., 2006a).

This program aims to reduce the incidence and prevalence of bovine tuberculosis (TB) by performing intradermal tests, culling positive animals, and detecting TB-like-lesions (TLL) in slaughterhouses as well as monitoring and controlling the transit of animals between different regions. In Brazil, the first program was launched in 2001 and was reviewed in 2016, when the epidemiological status of 13 states was described showing a heterogeneous herd prevalence among and within regions that ranged between zero and 13.9 % (LAGE et al., 2006b; FERREIRA NETO et al., 2016).

In recent years, the availability of a high number of records and high-quality data has helped to evaluate and improve animal disease surveillance programs in general (and bovine tuberculosis programs in particular) worldwide (MOUSTAKAS, 2017; VANDERWAAL et al., 2017b). In this sense, social network analysis (SNA) tools have been used to characterize cattle trade patterns and to identify highly connected premises that may act as hubs in the movement network. This can be useful to implement targeted control measures in order to reduce the incidence of communicable diseases such as TB, and especially in low prevalence regions

(VANDERWAAL et al., 2017a; MEKONNEN et al., 2019). However, the potential of this approach has not been assessed in Brazil yet. In this context, the Brazilian official veterinary service in particular has the necessary resources to approach the management of infectious diseases more efficiently using powerful tools like SNA (GONÇALVES; DE MORAES, 2017; SAVINI et al., 2017).

This study focusses on cattle trade from Rio Grande do Sul state (RS), Brazil, with a reported bovine population in 2018 of 12,451,432 animals, which represents the sixth largest population in the country and the largest in the southern region (IBGE, 2020). Most of the farms have a closed cycle (from breeding to fattening) and beef production is the predominant activity, followed by a mix of beef production and dairy production, and then sole dairy production. The last TB report in 2016, this state reported a herd prevalence of 2.8% (95% confidence interval (CI): 1.8, 4.0), and animal prevalence of 0.7% (95% CI 0.4%, 1%) (QUEIROZ et al., 2016).

The main control strategy for TB in RS is based on post-mortem inspection at the slaughterhouse, where a visual and manual examination of the carcass is conducted along with incisions of a defined range of tissues subjected to further visual examination in order to detect possible TLL.

In this region, active surveillance using the intradermal tuberculin test is not mandatory, and this test is generally applied for voluntary certification of free breeding establishments for brucellosis and tuberculosis in the frame of the PNCEBT program. Therefore, the detection of TLL plays an important role in the detection and control of TB in the population (MAPA, 2017).

Risk-based surveillance focuses on the subset of the population with a higher risk of infection; thus, the sensitivity of the surveillance system sensitivity reduces funding and labor costs. Hence, the modeling of TB through the space and network trade can help to design risk-based surveillance activities, especially in the case of TB, since a primary way of spread is the introduction of infected cattle through cattle movements (GILBERT et al., 2005; GREEN et al., 2008; PALISSON; COURCOUL; DURAND, 2016; VANDERWAAL et al., 2017a).

Transmission models based on network movements allow simulation of disease spread and can therefore be useful on the evaluation of control measures targeted to

specific highly connected premises to ultimately estimate the transmission chain and the potential number of affected herds (CHRISTEN et al., 2018). However, network-based modeling approaches for TB are challenging in part due to the long latent periods, low within-premises transmission rates, and limitations of diagnostic tests (VANDERWAAL et al., 2017a; BIRCH; GODDARD; TEARNE, 2018).

Therefore, to accurately estimate between-premises spread of TB, transmission models must run over long time periods and incorporate within-premises dynamics, including changes in within-premises prevalence over time to provide comprehensive quantitative representations of disease transmission pathways (VANDERWAAL et al., 2017a; PICASSO-RISSO et al., 2020).

The aims of this study were: i) to characterize the cattle trade in RS state in Brazil from 2016 to 2018 describing the static full, yearly and monthly snapshots of the network contact trade, ii) to identify clusters of TLL-positive premises in the spatial and movement networks as a proxy of the likelihood of spatial or movement-mediated TB transmission, and iii) to evaluate the potential of TB spread and targeted control actions using a Susceptible-Occult-Reactive-Infectious network model to inform the risk-based TB surveillance.

2. METHODOLOGY

2.1 Datasets description

Records of animal movements from RS state in Brazil were provided by the official veterinary service of the state. The database included all cattle movements with origin and destination in Premises located in RS. For each movement the following information was available: origin and destination (IDs and longitude and latitude coordinates), date and purpose of the movement (see below).

The whole dataset included 1,482,920 movement records. Incomplete or incorrect data (movements with missing IDs, same origin and destination, duplicates) (n= 8,532) were removed prior to the analysis so that the final database included 1,474,388 movements. For the static, temporal network and k-test analysis (see below), movements to slaughterhouses (36.54%, n= 53,8804) were excluded as these were assumed to be epidemiological endpoints.

The births dataset included 733,008 records (premises id, date and number of animals) of cattle births. The reports of TB cases were reported from lesions suggestive of

infection by mycobacterias detected during the official inspection of the carcasses of bovines in slaughterhouses part of the municipal and state level official surveillance system in RS. All records were records from 2016-01-01 to 2018-12-31 and provided by Secretary of Agriculture, Livestock and Agribusiness of State of Rio Grande do Sul (SEAPA-RS).

2.2 Characterization of the study population and movement network

We mapped the density of premises that moved at least one animal (density of active nodes), animals (animal density), outgoing-movements (outgoing -movement density) and outgoing moved animals (moved animal density) by municipality using the area of the municipalities in Km^2.

In addition, we mapped the balance of animals at the municipality level, calculated as the ratio between incoming and outgoing animals from a specific municipality (animal balance). Finally, we mapped the total of TLL by municipality. All calculations involving movements excluded those directed to slaughterhouses.

2.3 Network analysis

We constructed contact networks in which premises were defined as nodes and movements between premises were considered edges. The consequent contact network A was based on the movements during the study period and was represented as directed ($\mathrm{Ai,j} \neq A_{ji}$), such that the origin (node i) and destination (node j) give each edge a specific direction. We described the static and the time series network using data from all years of study as well as by year. Parameters measured are described in Table 1.

Table 1. Description of network analysis terminology and metrics

Parameter	Definition	Reference
Nodes	The unit of interest in network analysis, for example, premises or slaughterhouses.	(WASSERMAN; FAUST, 1994)
Edge	Link between two nodes in the network.	

Degree (k)	Number of unique contacts to and from a specific premise. When the directionality is considered, the ingoing and outgoing contacts are defined: out-degree is the number of contacts originating from a specific premise, and in-degree is the number of contacts coming into a specific premise.	
Movements	The number of animal movements records over a certain period of time.	
PageRank	Google PageRank measure, a link analysis algorithm that produces a ranking based on the importance for all nodes in a network with a range of values between zero and one. The PageRank calculation considers the indegree of a given premise and the indegree of its neighbors	(BRIN; PAGE, 1998)
Betweenness	The extent to which a node lies on paths connecting other pairs of nodes, defined by the number of geodesics (shortest paths) going through a node.	
Clustering coefficient	Measures the degree to which nodes in a network tend to cluster together (i.e., if A → B and B → C, what is the probability that A → C), with a range of values between zero and one.	
Giant weakly connected component (GWCC)	Proportion of nodes that are connected in the largest component when directionality of movement is ignored.	(WASSERMAN; FAUST, 1994)
Giant strongly connected component (GSCC).	Proportion of the nodes that are connected in the largest component when directionality of movement is considered.	(WASSERMAN; FAUST, 1994)
Out-Going Contac chain (OCC)	The outgoing contact chain (OCC) quantifies the number of ‘downstream' premises that could potentially acquire infection from the *index* premise through outgoing animal movements, adhering to the chronological order of the movements.	(FIELDING et al., 2019; PAYEN; TABOURIER; LATAPY, 2019).

2.4 Static Network description

A static network $G = (V, E)$ consists of a set of nodes V and a set of edges E, where every edge connects a pair of nodes. In the considered network, edges have a direction given by trade. Mathematically, a network can be represented as an adjacency matrix $\mathbf{A}$ with elements $\mathbf{A}_{ij} = 1$ if there is an edge from node i to node j and $\mathbf{A}_{ij} = 0$ otherwise.

To characterize the static network, the parameters Graph density, number of nodes, number of edges, diameter, number of moved animals, GSCC size and percentage, GWCC size and percentage, clustering coefficient and mean of the shortest paths were summarized by year and for all period of study.

2.5 Components description

The real-world directed networks often exhibit a bow-tie structure used as a large-scale map of the world wide web (BRODER et al., 2000; PAYEN; TABOURIER; LATAPY, 2019) (see figure 5a) where the GWCC is divided into five categories with a central bulk defined as the giant strongly connected component (**GSCC**), where any node can reach any other node following a directed path; a component upstream to the GSCC, called **in-component (GIC)**, where nodes can reach nodes of the GSCC following a directed path, but cannot be reached by the nodes of the GSCC; reciprocally, some nodes are downstream to the GSCC: they can be reached from the GSCC following a directed path, but cannot reach it; these constitute the **out-component (GOC)**. The remaining nodes of the giant component are part of structures called **tendrils** (going out from the in-component without reaching the GSCC, or going in the out-component without coming from the GSCC) and **tubes** (connecting directly the in- to the out-component, without going through the GSCC) (BRODER et al., 2000; PAYEN; TABOURIER; LATAPY, 2019; KNIFIC et al., 2020).

The premises were grouped according to the type of component and the distribution of the number of out-going contact chain (OCC) for each node from all study period was calculated.

2.6 time-series network analysis

A temporal snapshots network was considered, $g = (V, E, T)$, where V is a set of nodes and E is a set of edges in each observation period T. Each edge in E is given by a triplet (i, j, T) and connects node i and node j at time T. To describe the temporal patterns over time, we used a monthly time-window or series of snapshots (HOLME; SARAMÄKI, 2012). The descriptive assessment of the temporal network snapshots was made with the same parameters described in the table 1.

2.7 Relationship between the observed network and the distribution of TB-like lesion cases.

To evaluate whether there was a significant relationship between the observed network, the spatial location of the premises and the distribution of cases (TLL) across the network, a permutation-based approach, the so-called k-test, was performed. In this test, the observed distribution of the TLL cases in the movement network and geographic space was compared independently with the expected under the null hypothesis of random distribution of cases in space and within the network (VANDERWAAL et al., 2016).

The null hypothesis was generated through 1,000 Monte Carlo simulations in which the cases in the network are permutated. Reallocation of premises was performed using a degree-swapping approach to preserve the overall degree distribution of premises while randomizing the locations of TLL-premises relative to one another; TLL-premises were randomly swapped with premises whose degree fell in the same quartile of the overall degree distribution, as observed elsewhere (VANDERWAAL et al., 2016; POZO et al., 2019). The k-test was performed considering premises located within 5 and 10 km distances and one step (k = 1) within the network and was run using the number of cases reported for each year separately and for the cumulative time period.

Besides, the presence of purely spatial clusters was assessed using the spatial scan statistic with the SaTScan™ software developed by Kulldorff (KULLDORFF, 1997). The number of animals with TLL in each premise was assumed to follow a Poisson distribution in which the total number of animals in each premises was the population at risk, and the observed number of cases falling into windows of increasing size was compared to the distribution of expected cases if the spatial distribution of cases

occurred at random (null hypothesis), for the control were used premises that sent animals to slaughterhouses and not reported TLL. The distribution and statistical significance of the clusters was assessed by means of Monte Carlo replication of data sets under the null hypothesis with 999 replications to ensure an adequate power for defining clusters (http://www.satscan.org).

2.8 Disease spread model

We used the modelling framework SimInf, described by Widgren et al. (2019), to simulate a potential disease spread on the network explicitly over time. For this we used a compartmental SORI model in which the animal population was divided into four mutually exclusive compartments: susceptible (S), occult (O), reactive (R) and infectious (I).

Occult O state is a latent period of duration λ_1 in which even though infected, animals are not detectable by antemortem bTB tests and are not infectious. The animals then progress to the reactive state (R) at a rate of $\frac{1}{\lambda_1}$. The reactive animals are not infectious but could be detected via skin testing. Reactive animals ultimately move into the infectious state (I) at a rate of $\frac{1}{\lambda_2}$ where λ_2 is the average duration of the reactive state R. The final compartment represents animals that become infectious (I) while remaining detectable by antemortem diagnostic tests (ÁLVAREZ et al., 2014; PICASSO-RISSO et al., 2020).

Once in the I stage animals were assumed to stay infectious until culled. Animals were allocated into metapopulations (premises) and assumed to move from S to O , R and I according to state-specific transition rates. Here, we assumed homogenous mixing population within the premises, where all animals have identical rates of TB-causing contacts. We ignored heterogeneities related to age, space or behavioral aspects.

The model simulated disease spread at two levels (local and global), with the local level working as a stochastic compartment model and formulated as a continuous-time Markov chain (CTMC). The Gillespie stochastic simulation algorithm (SSA) was applied to simulate the number of individuals within each compartment through time using a transition rate from $S \overset{\beta}{\rightarrow} O \overset{1/\lambda_1}{\longrightarrow} R \overset{1/\lambda_2}{\longrightarrow} I$ as

$$\frac{dS}{dt} = u_{i,t,} - \frac{\beta S_i I_i}{S_i + O_i + R_i + I_i} \quad (1)$$

$$\frac{dO}{dt} = \frac{\beta S_i I_i}{S_i + O_i + R_i + I_i} - \left(O_i \frac{1}{\lambda_1}\right) \quad (2)$$

$$\frac{dR}{dt} = \left(O_i \frac{1}{\lambda_1}\right) - \left(R_i \frac{1}{\lambda_2}\right) \quad (3)$$

$$\frac{dI}{dt} = R_i \frac{1}{\lambda_2} \quad (4)$$

in a specific time t (GILLESPIE, 1977). The global-level was incorporated assuming a directed temporal network $g = (V, E, t)$ using the day-to-day scheduled movements from January 1st 2016 to December 31st 2018, where the number of incoming and outgoing animals update the number of animals in a given node i at time t. The movements with destination to slaughterhouses were considered subtracting these animals from the simulations; the number of eligible animals to move within nodes were sampled randomly. To maintain a stable herd size, the number of new animals due to births $u_{i,t,}$ were incorporated using the day-to-day scheduled births based on the farm owners' declaration to the official surveillance system for each specific premises.

The number of animals present in each premise on December 2016 was considered the herd size. We found some premises with negative balance in the herd population after consider in/out animal movements within premises, births and deaths records. To correct this balance, the negative number of animals were restored before ran the model.

2.8.1 Model parameters

Since we do not have field data for RS or Brazil to calculate the parameters, we use parameters reported in models and studies of TB at the farm level. For the within premises transmission coefficient rate β (per cow and year), we used alternatively the following values: 2.23 (PEREZ et al., 2002), 2.76 (BARLOW et al., 1997; FISCHER et al., 2005; SMITH et al., 2013; ÁLVAREZ et al., 2014; VANDERWAAL et al., 2017a; VERTERAMO CHIU et al., 2019; PICASSO-RISSO et al., 2020) and 5.2 (BARLOW et al., 1997; FISCHER et al., 2005; VANDERWAAL et al., 2017a; PICASSO-RISSO et al., 2020). For the others transmission rates, we assumed λ_1 = 41 days (ALLEPUZ et al., 2011; ÁLVAREZ et al., 2014; O'HARE et al., 2014) and λ_2 = 6 months (BARLOW

et al., 1997; ÁLVAREZ et al., 2014; O'HARE et al., 2014; VANDERWAAL et al., 2017a; VERTERAMO CHIU et al., 2019).

To run the model, we considered two initial scenarios: the first one using 3,055 premises randomly sampled from the network in each simulation as infected. The second scenario was started considering as infected the 3,055 premises in which at least one animal had TB-like lesions reported at slaughterhouses during the 2016-2018 period. For both models the simulation assumed an initial within-premises animal prevalence of 7 % according with the intra-herd TB prevalence reported by (QUEIROZ et al., 2016).

2.8.2 Disease spread and targeted control action modeling

The models were run using 1000 replications of different targeted intervention measures by sequentially removing an increasing number from 1 to 25,000 nodes prior to the simulation based on network parameters rank: Degree, Betweenness, PageRank, and random nodes. All network-based parameters were calculated using the full contact network, and after each node-removal, the epidemic curve and prevalence were calculated and the reduction of the number of infected farms was calculated at the end of each simulated scenario (simulation day = 1095). Additionally, we also simulated a scenario in which no control measures at all were applied (No-control). To explore significant differences on the final number of infected farms, between scenarios the Kruskal-Wallis and Wilcoxon test followed by post-hoc tests using Bonferroni corrections was used.

2.8.3 Sensitivity analyses

Since we proposed a model with local and global dynamics the sensitivity analyses were discriminated in a local level were only one node was simulated; to include the vital dynamics the means of ingoing and outgoing animals were calculated from the movements data and expressed in a six-month rate, therefore, for each six months of simulation 7% of animals were added and removed according with the herd size, were used 1000 Latin Hypercube Sampling (LHS) to and 100 replications, and was considered the prevalence of the infected animals as the output model. For the global sensitivity considers contact network dynamics, births and deaths of animals (The

complete model) and the output model to consider was the number of infected premises at the end of simulations using 300 LHS and 100 replications.

Were select the parameters intervals for β (1 to 5.2) (PEREZ et al., 2002; ÁLVAREZ et al., 2014; VANDERWAAL et al., 2017a; PICASSO-RISSO et al., 2020), λ_1 (1/14.1 to 1/45) (ROSE; WALL, 2011; SMITH et al., 2013; ÁLVAREZ et al., 2014; VANDERWAAL et al., 2017a; PICASSO-RISSO et al., 2020), λ_2 (1/180 to 1/630) (BARLOW et al., 1997; ROSE; WALL, 2011; SMITH et al., 2013; ÁLVAREZ et al., 2014; VANDERWAAL et al., 2017a; PICASSO-RISSO et al., 2020) and, for the local sensitivity analysis also were considered the herd size (10 to 1000 animals); for all parameters were used the LHS to explore the parameters space (YANG et al., 2017) and the Partial rank correlation coefficients (PRCCs) to measure the strength of correlations. A positive PRCCs value indicates that the value of the model output can be increased by increasing the respective model input parameter, and the model output can be decreased by forcing down the relative input parameter. Otherwise, a negative PRCCs value indicates a negative correlation between the model input and output (YANG et al., 2017; BIDAH; ZAKARY; RACHIK, 2020; NABI, 2020). In general, the PRCCs-LHS provides a measure of monotonicity between a set of parameters and the number of infected animals after removal of the linear effects of all parameters except the parameter of interest (MARINO et al., 2008; GUO et al., 2020).

2.9 Software

The software used for analysis and graphics was R statistical software (versions 3.6) (R CORE TEAM, 2017) with RStudio editor using the packages: igraph 1.2.4 (NEPUSZ, 2006), tidyverse 1.2.1 (WICKHAM et al., 2019), SimInf 6.3.0 (WIDGREN et al., 2019), sf 0.5-3 (PEBESMA, 2018), and brazilmaps 0.1.0 (PRADO SIQUEIRA, 2017), incidence (KAMVAR et al., 2019) and for the spatial cluster analysis was used SaTScan™ software (JUNG; KULLDORFF; RICHARD, 2010).

3. RESULTS

3.1 Characterization of the study population and movement network

The municipalities with the largest number of premises (3 to 4.51 premises/ Km2) were located in the northern and in the central-western parts of the state near the metropolitan region of Porto Alegre (Figure 1a).

The higher number of outgoing movements was localized in the southwestern part of the state, with zero to 20 cattle movements/ Km2 (green to yellow areas in Figure 1b), and there was also a hotspot in the central-western part with 24.19/ Km2 outgoing movements.

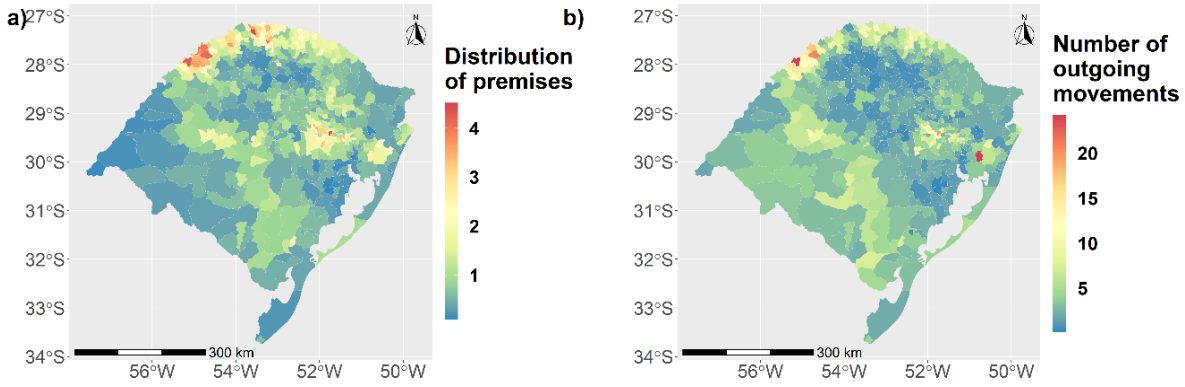

Figure 1. Spatial distribution of premises and animal movements in RS state. a) Distribution of premises in Km^2 by municipalities. **b)** Number of outgoing movements in Km^2 by municipalities.

The number of animals by Km^2 showed a heterogeneous distribution, with a higher cattle population in the southwestern part of the state (60 to 115 animals/ Km^2) (figure 2a). This region also had the highest number of moved animals (46 to 392 moved animals/ Km^2) (figure 2b). In general, the cattle trade had a neutral ingoing/outgoing balance in the total number of the animals traded, with the exception of the south-west region, which exported more than they imported, and two municipalities with more than 300,000 imported animals (Figure 2c).

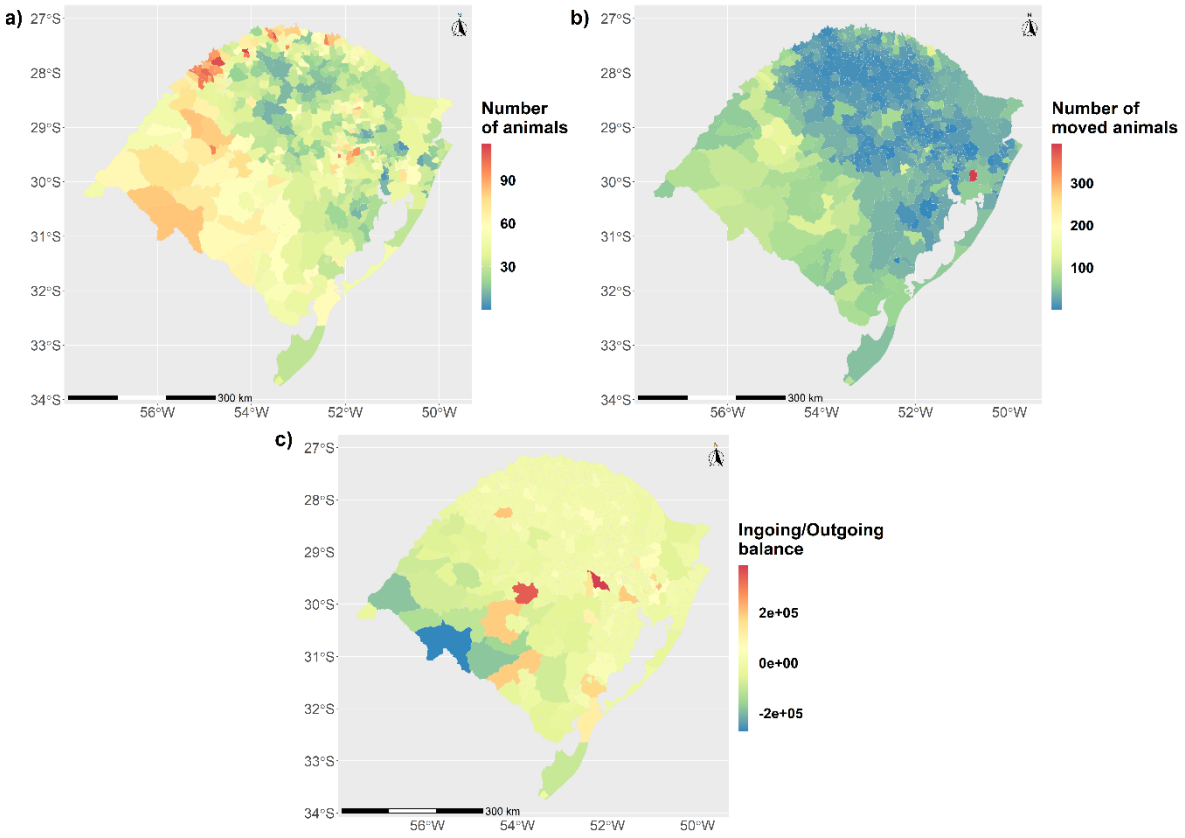

Figure 2. Spatial distribution of animals, premises, animal and ingoing/outgoing balance in RS state. a) Herd size by municipalities by $Km^{2.}$ **b)** Number of outgoing number of animals in Km^2 by municipalities. **c)** Balance between ingoing/outgoing total number of animals.

All animal movements were grouped in six purpose categories: movements of animals to fattening units (**Fattening)** with 56.7% of the movements**,** animals destined for a Semen Collection and Processing Center, as well as animals destined for natural breeding on a specific property, or other reproductive activities (**Reproduction)** with 5.62%, movements to slaughterhouses (**Slaughterhouses)** with 36.7 %, movements to or from events or fairs (to **Events** (0.03%) and **return from events** (0.06%)**,** respectively), and movements for other purposes (veterinary care, weighing, etc., **Others** (0.086%)). The monthly number of movements by purposes are depicted in the supplementary figure 1.

3.2 Static Network description

The annual number of nodes, edges and animals and the estimates for network parameters graph density, GSCC, GWCC throughout the 3-year span are shown in

Table 2. The number of animals moved increased over the years but no trend in the number of edges was observed over the study period. Despite the observed decrease in the number of nodes, an increase in graph density was detected. The increase in the diameter of the network together with the mean of shortest paths showed a more connected network year by year (table 2).

Table 2. Static network description. Network parameters of RS state by year and for all years.

Year	Nodes	Edges	Animals	Graph density	Diameter	GSCC (%)	GWCC (%)	Clustering Coefficient	Mean shortest paths
2016	158,469	316,455	4,809,197	1.26E-05	40	29,148 (18.39)	133,069 (83.97)	0.021	10.71
2017	151,498	307,943	4,960,304	1.34E-05	45	27,326(18.04)	125,685 (82.96)	0.020	10.29
2018	149,754	314,282	5,030,184	1.40E-05	35	26,797 (17.89)	126,709 (84.61)	0.017	9.86
All years	237,436	938,680	14,799,685	1,67E-05	32	86,315 (36.35)	223,086 (93.96)	0,025	8.13

3.2.1 Components analysis

To represent the results, the static network was depicted using a so-called bow-tie partition (Figure 3a) where nodes are classified into four different components; (GIC), giant out component (GOC), Tubes & tendrils, and isolated components, the figure 5a shows the number and proportion of the different components with the tube & tendril component showing the highest size (40.7%) followed by the GSCC component (36.35%). The size of the GWCC was 223,086 and represented 93% of the network.

We calculated the reachability of the directed network using the thought-full static network components description. The spreading potential was calculated using the size of the outgoing contact chain in each component in the network, the GIC and GSCC showed a higher out going contact chain distribution compared with GOC and isolated, the Tubes & tendril has a lower distribution despite a higher number of outliers (Figure 3b).

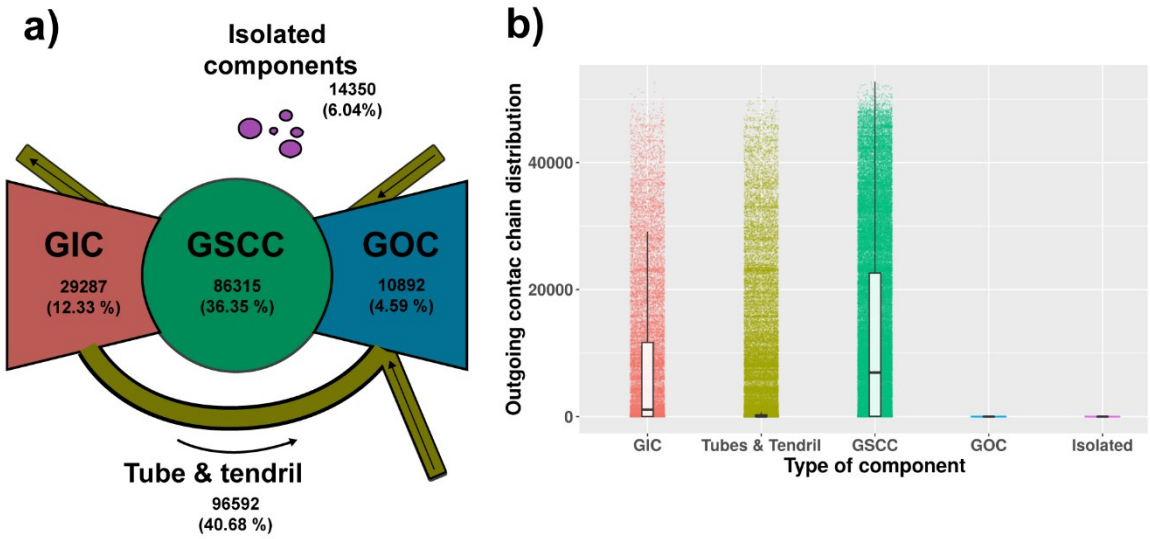

Figure 3. a) Bow-tie structure of a directed graph. The GWCC was separated into GSCC, the relative in and out-components, tendrils, and tubes. Adapted from (BRODER et al., 2000; PAYEN; TABOURIER; LATAPY, 2019). **b)** Each little point represents the outgoing contact chain distribution by type of component for all study periods, the white boxes represent a boxplot of components distributions.

3.3 Time-series network description

When the network parameters were analyzed on a monthly basis, a seasonal trend was observed, with marked maximum and minimum values especially for the months 5 and 11 (May and November). The number of animals, graph density and GSCC/GWCC were strongly influenced by the decreasing number of nodes and edges (Figure 4).

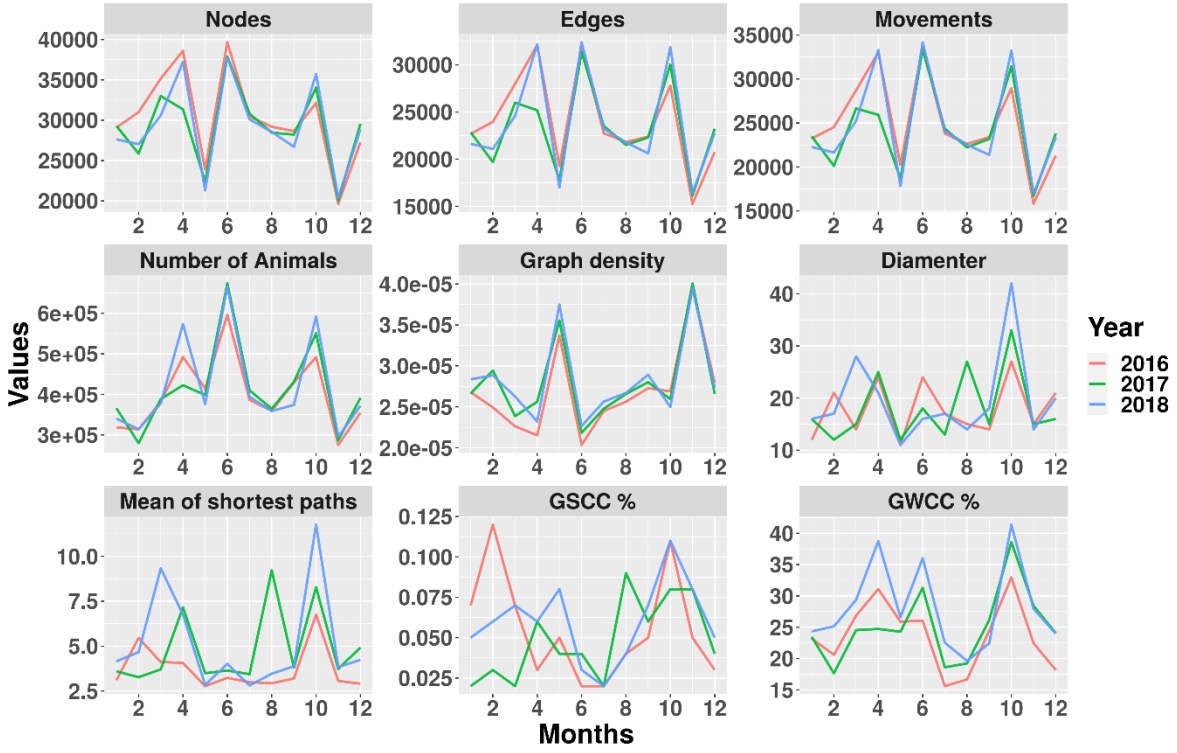

Figure 4. Description of the network using a time-aggregate windows of 30 days from the parameters: Nodes, Edges, movements, Number of animals, Graph density, Diameter, mean of the shortest paths, GSCC and GWCC; the description of parameters are shown in Table 1.

3.4 Relation between the observed network and the distribution of cases across the network

The k-test showed significant clustering of TB-like lesion locations both in the annual (supplementary figures 2 -3) and cumulative networks (figure 5). Premises with TB-like lesions were connected to an annual mean of 2.07, 2.44 and 2.68 positive premises in 2016, 2017 and 2018 respectively, and 5.92 for the cumulative years. These values were significantly (p-value < 0.001) higher than what would be expected under the null hypothesis of random distribution of lesions across the network. The observed number of premises including animals with TB-like lesion located within 5 and 10 kilometers of other premises (annual ranges of 3.80-4.01 and 9.48-10.07, respectively) was also significantly greater ($p < 0.001$) than what would be expected if premises were distributed randomly in space.

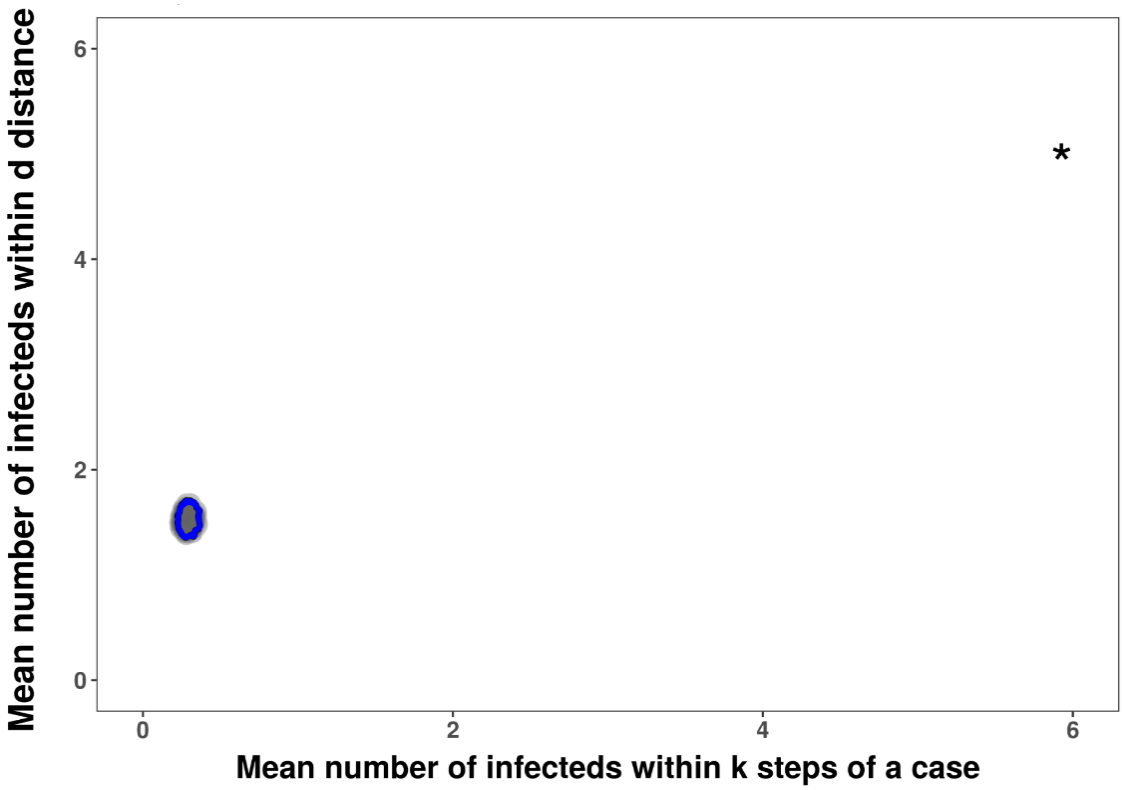

Figure 5. Graphical results of the k-test for the cumulative network considering a threshold of 5 km and k=1 step in the network. The star indicates the observed mean of positive premises within 1 step in the network (x-axis) and positive premises within 5 km (y-axis). The grey-shaded region represents the null distribution of the k-statistic when positive premises were randomly distributed within the network. Blue line represents the 95% of the null distribution of positive premises within one step in the network.

3.5 Spatial distribution and cluster analysis

We build a map with the prevalence by productive zones according with reported by Queiroz et.al 2016 depicted in Figure 6a, and compare with the cluster founded with the spatial distribution of the premises from which 2,945 animals with TLL (farms with available geolocation of 3,055 cases) figure 6b.

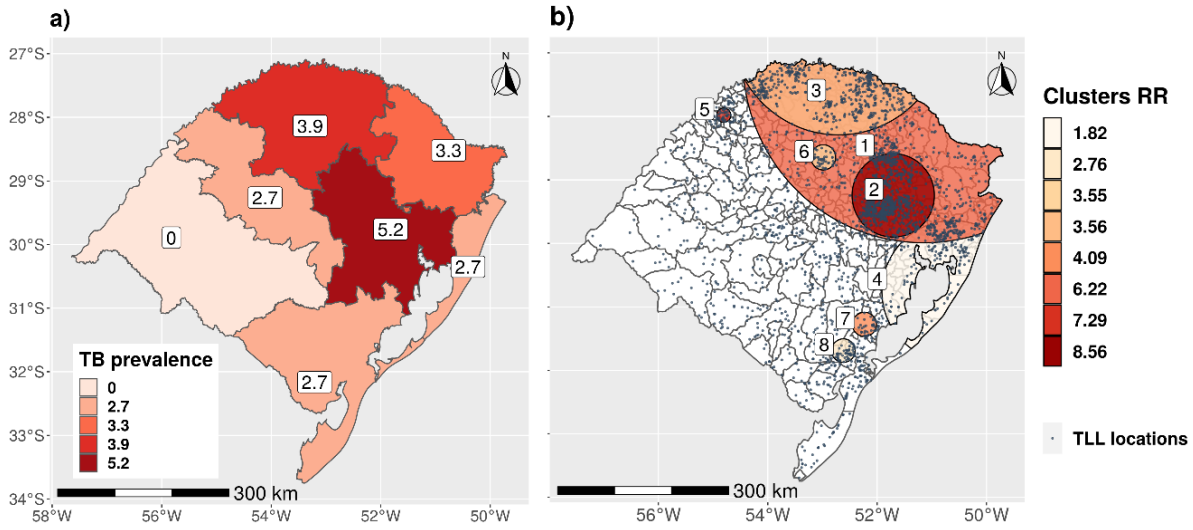

Figure 6. a) Map of prevalence of TB by productive regions in RS (Adapted from Queiroz et.al 2016). **b)** Clusters of TLL locations (premises with reported TLL) for the RS state for all study period and the blue dots represents the premises locations.

The results of the cluster spatial analysis are shown in Table 3 and Figure 6b. Seven significant spatial clusters were found in the state. These clusters were located in the northern and eastern part of the state with radius ranging between 12.5 to 323.17 km and relative risks between 1.82 and 8.56.

Table 3. Significant high rate TLL spatial clusters in Rio Grande do Sul area.

Cluster	Radius (km)	No. of herds in cluster	No. of cases in cluster		Relative Risk	p-value
			Observed	Expected		
4	123.55	3,629	257	146.91	1.82	3.18E-11
8	20.47	418	52	19.1	2.76	0.000152
6	21.95	1,406	43	12.23	3.55	3.44E-06
3	197.9	21,766	517	167.34	3.56	1.00E-17
7	21.04	1,180	30	7.39	4.09	0.000134
1	328.17	55,109	1854	662.12	6.22	1.00E-17
5	12.5	1,134	32	4.43	7.29	3.52E-11
2	73	15,744	801	124.82	8.56	1.00E-17

3.6 Disease spread modeling

Results of two different sets of scenarios after 1000 model replications are described: the first one corresponds to the scenario in which no control measures are simulated (No-control). This was the scenario leading to, the largest increase in the number of infected premises at the end of the simulated period, from 3,055 herds to between 10,323- and 19,480 when the infection was seeded in random premises (Figure 7) and between 10,664 and 19,836 when infection was seeded in TLL positive premises (supplementary Figure 5).

In the second set of scenarios, when control actions based on network metrics (removal of 25,000 nodes based on the different network metrics) were simulated, a larger impact (i.e., decrease in the number of infected premises over time compared to the No-control scenario) was observed when nodes were removed based on higher degree followed by PageRank and betweenness, while removal of randomly selected nodes showed the lowest impact as expected, with a result very close to a baseline scenario. These patterns were similar regardless of whether the infection was seeded in randomly chosen case premises (Figure 9) or TLL positive premises (supplementary Figure 4).

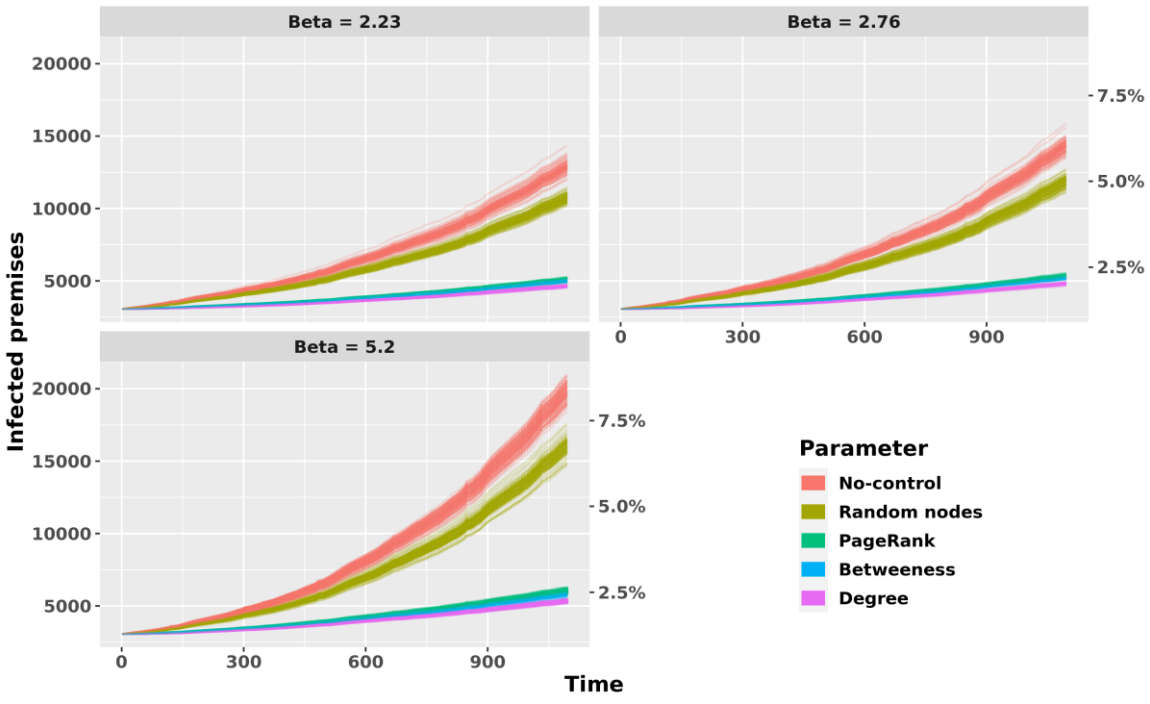

Figure 7. Predicted infection curves controlling by network-based control actions and without control action (No-control) in the temporal network representation of cattle

movements for different probabilities of transmission (1, 2.76 and, 4.13) using 3050 random nodes as initial infected premises in each simulation. The Y- left axis represents the total of infected premises at the end of simulation, and the y-right represent the percentage of infected premises. The x-axis represents the simulation time in days.

When the prevalence in the last day of simulation (day =1,095) obtained in the different scenarios was assessed, similar results were observed, and again removing nodes based on degree had again the largest impact on the infected number of premises across all transmission coefficients considered. A higher performance of the control strategy when removal was based on degree compared with the others SNA parameters ($p<0.001$, Kruskal-Wallis test and Dunn pos-hoc with Bonferroni corrections). Similarly, removal of nodes based on PageRank and betweenness showed also higher performance in reducing the prevalence more than 50% (Figure 8 for randomly seeded case herds, Suppl. Fig 5 for infection seeded in TLL-positive premises).

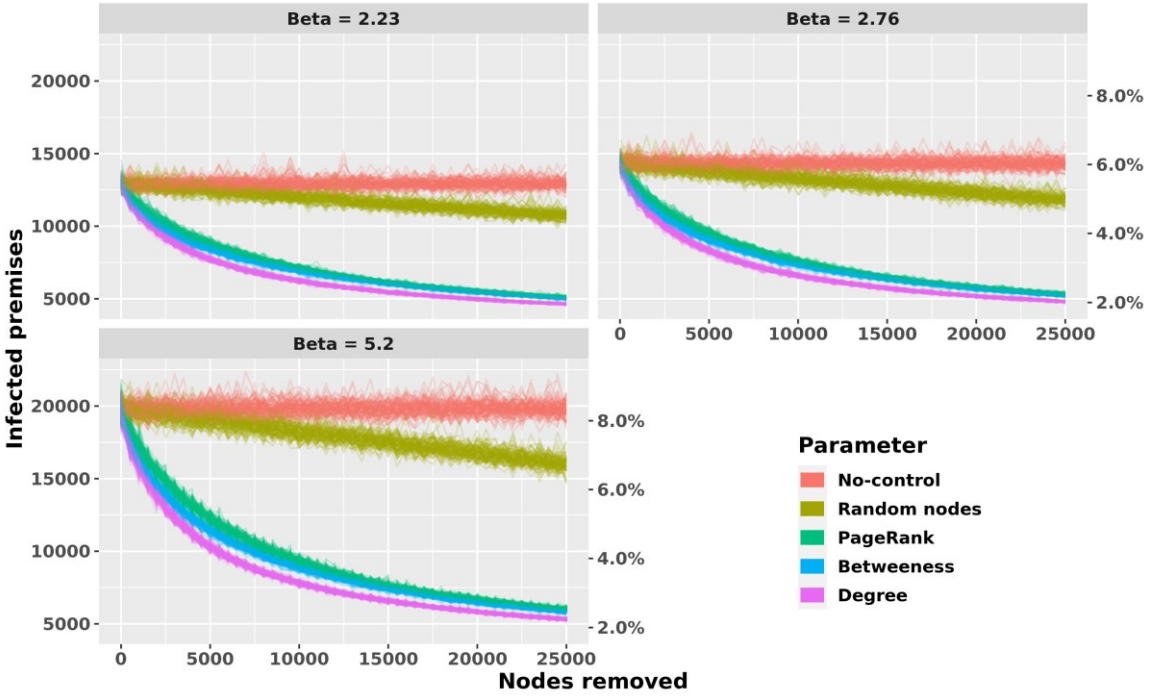

Figure 8. Node removal model in RS state based on the transmission rates (1, 2.76, and, 4.13) and network parameters: PageRank, betweenness degree, and random nodes from 100 model interaction using 3,050 random nodes as initial infected premises in each simulation. The Y- left axis represents the total of infected premises

at the end of simulation, and the Y-right represent the percentage of infected premises. The x-axis represents the simulation time in days.

3.6.1 Sensitivity analyses

For the local model sensitivity 1000 LHS were replicated 100 times were considering the parameters (β, $1/\lambda_1$, $1/\lambda_2$, and herd size) and the output model was the prevalence of infected animals where the parameter with the highest positive influence was for β followed by $1/\lambda_2$, slice size and $1/\lambda_1$, respectively; herd size showed a negative correlation. All intervals in the PRCCs were very small. the results were represented graphically in figure 9 and supplementary figure 6.

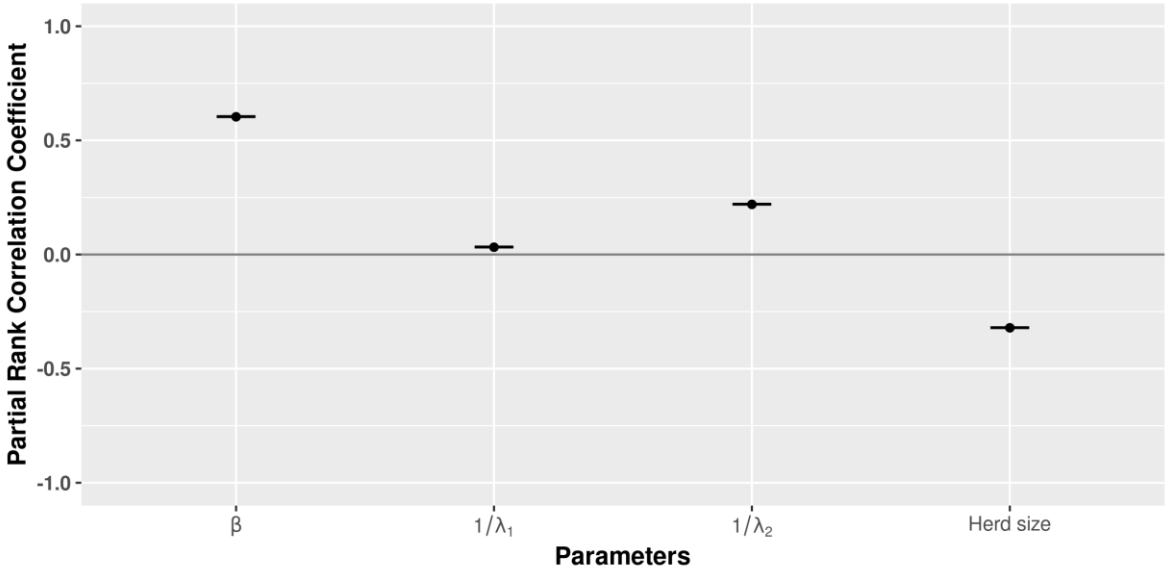

Figure 9. LHS-PRRC local sensitivity results for 1000 samples and 100 replicates for parameters β, $1/\lambda_1$, $1/\lambda_2$, and herd size with a PRCC significantly ($p < 0.05$).

In the global model sensitivity, the β parameter presented a greater influence on the number of infected farms at the end of the simulation, the other parameters maintained similar patterns to the local sensitivity, the complete results are described in figure 10 and explained in the supplementary figure 7.

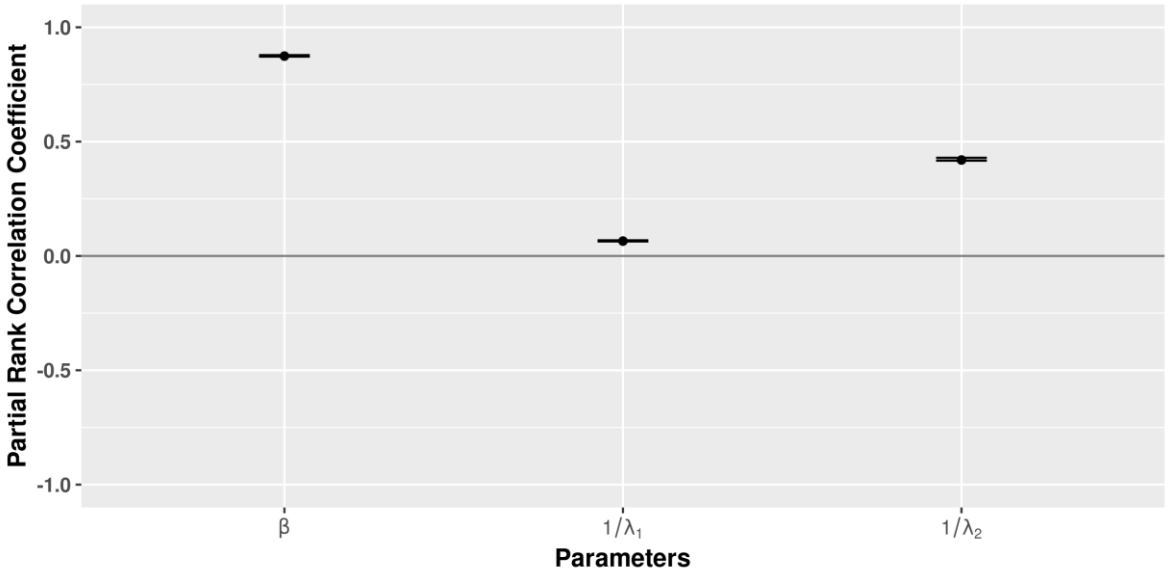

Figure 9. LHS-PRRC global sensitivity results for 1000 samples and 100 replicates for parameters β, $1/\lambda_1$, $1/\lambda_2$, and herd size with a PRCC significantly ($p < 0.05$).

The assessment of the number of infected premises when just one parameter (for β, λ_1, or λ_2) was perturbed while the others remained fixed demonstrates a strong impact of all three in the predictions, with overall simulated prevalence values ranging between 3.71% and 8.01% depending on the parameter, the β parameter showed the highest widespread intervals of the final range prevalence, in addition, a wider range as also observed for the parameter λ_2 this can be expected due to the higher range of this parameter (from 3 to 21 months) all results are depicted in the supplementary figure 8.

4. DISCUSSION

This work explored the cattle trade and their relation with TB. To solve this, the static network, density of animals, movements were described. Besides, monthly snapshots were generated to represent the temporal trends in the network over time to give an overview of the cattle trade in the RS state.

Afterwards, we explored and established a plausible association between animal movement with geographical and cluster proximity in the creations of epidemiological links between positive TLL premises. Based on these results was evaluate the possible TB spread using a SORI model on the studied network and we used this model to

explored network-based targeted surveillance and controls action for TLL in RS state in Brazil.

The use of the static and time-series snapshot network was aimed to provide an overview of the topology and structure of the network. In the RS state, the surveillance system is based on intervention at the municipality level. For this reason, we described the spatial patterns at the municipality level. However, to avoid the possible distortion due to the heterogenous size of the municipalities, we adjusted the results considering a density in Km^2. This analysis showed a higher concentration of premises in the northwest part of the state but a higher number of movements and animals in the south part; these patterns are probably due to the higher herd sizes of premises in the southwest and southeast part of the state compared with the other regions. This is particularly important because these regions share a large frontier with Uruguay and Argentina, and these south regions were also identified as risk areas for foot and mouth disease (SANTOS et al., 2017).

When we explored the monthly temporal network, we found a clear temporal trend between May and November, when the trade activity decreased considerably. These changes over time can be explained by the vaccination campaigns against foot and mouth disease, which are applied during these months when many batches are confined for the count and vaccination (LAGE et al., 2006a).

We explored the connected components using a bow-tie description as adopted by (PAYEN; TABOURIER; LATAPY, 2019). This structure can be used as a proxy of the potential risk of spread due to certain premises according to their location in the bow-tie structure. As expected, the GSCC showed a higher spread potential considering the OCC distribution (Fig. 5) despite the lower number of premises in the GIC (12.33% of the network), Tubes & tendrils also showed higher outlier values of OCC, but it is worth noting that this component also has a greater number of Premises on the network (40.68% of the network);The premises at the end of the commercial trade were allocated in the GOC showing lower OCC values.

We explored the distribution of the TLL positive Premises over components and we found 61.93 % of the cases in the GSCC, this could explain in part the higher values in the SORI model simulation when these TLLs were used as index cases (supplementary figure 5-6), followed by Tube & tendril, GOC, GIC, and isolated with

16.63%, 5.67%, 5.19%, and 1.01% respectively. Therefore, a large percentage of cases have a high potential to be disease spreaders.

Considering these results, we calculated whether the pattern of TLL cases within the observed contact network was likely to have resulted from transmission through animal movements or through contact between neighboring premises. The k-test showed a significant association between TLL positive premises and the structure of the network in the network of each year (2016 to 2018) and the full period, so that premises with animals with TLL tended to be closer in the network over the expected values. This association was also present in the space using threshold distances of 5 and 10 km, so that premises with TLL animals were closer in space than expected, similar results were obtained in Uruguay (VANDERWAAL et al., 2016) where a large bonder frontier are shared with RS.

The results of the local spatial clustering analysis confirmed these results, and identified eight clusters (with relative risks ranging between 1.8 and 8.6). These high risk zones are largely consistent with areas with a high TB prevalence in RS reported in 2016 (QUEIROZ et al., 2016)(see figure 6). Several factors could explain this apparent higher risk in the spatial clusters, including different herd sizes (herds in risk areas were significantly (Mann-Whitney test, $p<0.01$) smaller (median = 16 animals) than those outside of risk areas (median = 80 animals)), this could be associated with different management of premises, and higher density of animals and premises (Figures 2a-2b) specially for daily cattle.

Since we showed the association between TLL positive premises in the network, a SORI model was used to evaluate the possible spread of the infection through cattle movement under the premise of no testing and no movements restrictions, and the impact of several control actions based on removal of certain nodes according to their relevance in the network. Once we simulated the removal of 15,000 nodes (6.6 % of all nodes in the network) based on Degree, Betweenness and PageRank, we obtained a reduction in the prevalence at the end of the study period of around 50% for all transmission rates. These results agree with others node remotion-models based on network approaches using network fragmentation of the connected components in Italy, Great Britain and Cameroon suggesting the SNA parameter degree as important control measure for scale free networks (NATALE et al., 2009; GATES;

WOOLHOUSE, 2015; MOTTA et al., 2017). The number of infected premises at the end of simulation when seeding the infection in farms with TLL were higher than the simulations using random nodes these results can be explained in part due 56% of the TLL positive premise are in the GSCC of the network thus these premises have more reachability.

We want to explore the influence of the network in the simulations if the order of the movements chance randomly over time (methodology detailed in the supplementary material), for that reason we used a permuted network to change these movements order. The results showed a significant increase in the number of infected premises in the permuted networks (p-value <0.001) with a median of the prevalence in 6.4% and 5.9 for real-data simulations suggesting that the infection curves are highly dependent on the order of the connections despite the degree distribution, results are showed in the supplementary figure 9.

In this study, data on the confirmation of laboratory results was not available, and therefore we could not be completely sure that farms with TLL animals were truly infected. Moreover, given the lack of ante-mortem test results in all farms and limitations in the sensitivity of abattoir surveillance (WILLEBERG et al., 2018), other farms could have been infected but remain undetected.

For these reasons, we selected random premises as cases as our starting point in part of our modeling exercises. Interestingly, the patterns in the results were relatively similar to those obtained when seeding the infection in farms with TLL animals, although a much larger variability in the results was observed as expected, suggesting that the initial farms being infected could in fact impact the outcome of the transmission over a three-year period.

Nevertheless, in a study conducted in 2015 in RS, the Comparative Cervical Test revealed a 26.4% of reactors and 13.2% of inconclusive animals in 53 dairy cattle premises. At slaughter, TB-like lesions were found in tissues of 92.9% and 71.4% of the reactor and inconclusive animals (RODRIGUES et al., 2017), indicating that the use of TLL can be a good proxy of the infected animals in this region.

Therefore, we are confident that this work provides useful information for the control and eradication program of tuberculosis of the Brazilian government (PNCEBT). For

this work, we were not able to determine the number and the impact of illegal or unreported movements, so it was assumed that the spread of infection was only due to known movements neglecting other potential pathways as movements of others species susceptible to TB, movement of owners, workers or veterinarians, direct contact between neighboring farms (fence-to-fence contact) and transmission via fomites (KNIFIC et al., 2020). Thus, the control of TB and other infectious diseases must be analyzed in conjunction with other epidemiological tools and approaches.

5. CONCLUSION

The characterization of the network provided detailed information to understand the cattle trade, spatial patterns and describe the temporal trading fluctuations, suggesting that surveillance activities should consider the spatiotemporal variation. This network characterization may result valuable to quantify the network-associated risk for other transmissible diseases through cattle movements. There was a significant relationship between the observed network, the spatial location of the premises, and the distribution of cases (TLL), so tracking origin and destination of animals from TLL positive premises can be useful to detect more TLL in the network. The SORI model developed can be used to estimate the epidemic sizes of TB in RS state considering the contact trade, may help to determine the network metrics that should be selected for the risk-based selection of target premises according to the approximation of epidemic sizes, and it is useful to evaluate the impact of node removal to calculate the minimum number of premises to be targeted.

6. References

ALLEPUZ, a et al. Analysis of the spatial variation of Bovine tuberculosis disease risk in Spain (2006-2009). **Preventive veterinary medicine**, v. 100, n. 1, p. 44–52, 1 jun. 2011. Disponível em: <http://www.ncbi.nlm.nih.gov/pubmed/21429605>. Acesso em: 21 out. 2014.

ÁLVAREZ, J. et al. Bovine tuberculosis: Within-herd transmission models to support and direct the decision-making process. **Research in Veterinary Science**, v. 97, p. S61–S68, out. 2014. Disponível em: <http://www.sciencedirect.com/science/article/pii/S0034528814001404>.

BAJARDI, P. et al. Dynamical Patterns of Cattle Trade Movements. **PLoS ONE**, v. 6, n. 5, p. e19869, 18 maio 2011. Disponível em: <https://doi.org/10.1371/journal.pone.0019869>.

BAJARDI, P. et al. Optimizing surveillance for livestock disease spreading through animal movements. **Journal of The Royal Society Interface**, v. 9, n. 76, p. 2814–2825, 7 nov. 2012. Disponível em: <http://rsif.royalsocietypublishing.org/content/early/2012/06/21/rsif.2012.0289.abstract>.

BARLOW, N. D. et al. A simulation model for the spread of bovine tuberculosis within New Zealand cattle herds. **Preventive Veterinary Medicine**, v. 32, n. 1–2, p. 57–75, set. 1997. Disponível em: <http://www.sciencedirect.com/science/article/pii/S0167587797000020>.

BIDAH, S.; ZAKARY, O.; RACHIK, M. Stability and Global Sensitivity Analysis for an Agree-Disagree Model: Partial Rank Correlation Coefficient and Latin Hypercube Sampling Methods. **International Journal of Differential Equations**, v. 2020, p. 1–14, 1 abr. 2020. Disponível em: <https://doi.org/10.1155/2020/5051248>.

BIRCH, C. P. D.; GODDARD, A.; TEARNE, O. A new bovine tuberculosis model for England and Wales (BoTMEW) to simulate epidemiology, surveillance and control. **BMC Veterinary Research**, v. 14, n. 1, p. 273, 4 dez. 2018. Disponível em: <https://doi.org/10.1186/s12917-018-1595-9>.

BRIN, S.; PAGE, L. The anatomy of a large-scale hypertextual Web search engine. **Computer Networks and ISDN Systems**, v. 30, n. 1–7, p. 107–117, abr. 1998. Disponível em: <http://dx.doi.org/10.1016/S0169-7552(98)00110-X>.

BRODER, A. et al. Graph structure in the Web. **Computer Networks**, v. 33, n. 1–6, p. 309–320, jun. 2000. Disponível em: <http://www.sciencedirect.com/science/article/pii/S1389128600000839>.

CHRISTEN, A. et al. Modeling a SI epidemic with stochastic transmission: hyperbolic incidence rate. **Journal of Mathematical Biology**, v. 76, n. 4, p. 1005–1026, 27 mar. 2018. Disponível em: <https://doi.org/10.1007/s00285-017-1162-1>.

FERREIRA NETO, J. S. et al. Analysis of 15 years of the National Program for the

Control and Eradication of Animal Brucellosis and Tuberculosis, Brazil. **Semina: Ciências Agrárias**, v. 37, n. 5Supl2, p. 3385, 9 nov. 2016. Disponível em: <http://www.uel.br/revistas/uel/index.php/semagrarias/article/view/27292>.

FIELDING, H. R. et al. Contact chains of cattle farms in Great Britain. **Royal Society Open Science**, v. 6, n. 2, p. 180719, 28 fev. 2019. Disponível em: <doi.org/10.1098/rsos.180719>.

FISCHER, E. A. J. et al. Evaluation of surveillance strategies for bovine tuberculosis (Mycobacterium bovis) using an individual based epidemiological model. **Preventive Veterinary Medicine**, v. 67, n. 4, p. 283–301, mar. 2005. Disponível em: <http://www.sciencedirect.com/science/article/pii/S0167587704002314>.

GATES, M. C.; WOOLHOUSE, M. E. J. Controlling infectious disease through the targeted manipulation of contact network structure. **Epidemics**, v. 12, p. 11–19, set. 2015. Disponível em: <http://www.sciencedirect.com/science/article/pii/S1755436515000304>.

GILBERT, M. et al. Cattle movements and bovine tuberculosis in Great Britain. **Nature**, v. 435, n. 7041, p. 491–496, maio 2005. Disponível em: <http://www.nature.com/articles/nature03548>.

GILLESPIE, D. T. Exact stochastic simulation of coupled chemical reactions. **The Journal of Physical Chemistry**, v. 81, n. 25, p. 2340–2361, 1 dez. 1977. Disponível em: <https://doi.org/10.1021/j100540a008>.

GONÇALVES, V. S. P.; DE MORAES, G. M. The application of epidemiology in national veterinary services: Challenges and threats in Brazil. **Preventive Veterinary Medicine**, v. 137, p. 140–146, 1 fev. 2017. Disponível em: <http://www.sciencedirect.com/science/article/pii/S016758771630633X>.

GREEN, D. M. et al. Estimates for local and movement-based transmission of bovine tuberculosis in British cattle. **Proceedings of the Royal Society B: Biological Sciences**, v. 275, n. 1638, p. 1001–1005, 7 maio 2008. Disponível em: <https://doi.org/10.1098/rspb.2007.1601>.

GUO, Z. et al. An artificially simulated outbreak of a respiratory infectious disease. **BMC Public Health**, v. 20, n. 1, p. 135, 30 dez. 2020. Disponível em:

<https://doi.org/10.1186/s12889-020-8243-6>.

HOLME, P.; SARAMÄKI, J. Temporal networks. **Physics Reports**, v. 519, n. 3, p. 97–125, out. 2012. Disponível em: <https://linkinghub.elsevier.com/retrieve/pii/S0370157312000841>.

IBGE. **Banco de tabelas estatisticas - Instituto Brasiliro de Geografia e Estatistica Brazil**. Disponível em: <https://sidra.ibge.gov.br/home/pms/brasil>. Acesso em: 17 ago. 2020.

JUNG, I.; KULLDORFF, M.; RICHARD, O. J. A Spatial Scan Statistic for Multinomial Data. **Statistics in Medicine**, v. 29, n. 18, p. 1910–1918, 7 maio 2010. Disponível em: <https://pubmed.ncbi.nlm.nih.gov/20680984>.

KAMVAR, Z. N. et al. Epidemic curves made easy using the R package incidence. **F1000Research**, v. 8, n. 139, p. 139, 31 jan. 2019. Disponível em: <http://openr.es/f6w>.

KNIFIC, T. et al. **Implications of Cattle Trade for the Spread and Control of Infectious Diseases in Slovenia Frontiers in Veterinary Science** , 2020. . Disponível em: <https://www.frontiersin.org/article/10.3389/fvets.2019.00454>.

KULLDORFF, M. A spatial scan statistic. **Communications in Statistics - Theory and Methods**, v. 26, n. 6, p. 1481–1496, 27 jan. 1997. Disponível em: <https://doi.org/10.1080/03610929708831995>.

LAGE, A. et al. Programa nacional de controle e erradicação da brucelose e da tuberculose animal (PNCEBT). **Brasília: Ministério da**, 2006a.

LAGE, A. P. et al. **Programa Nacional de Controle e Erradicação da Brucelose e da Tuberculose (PNCEBT)**Brasília, MAPA/SDA/DSABrasil. Ministério da Agricultura Pecuária e Abastecimento. Animal, , 2006b. .

MAPA. **regulamento tecnico -Ministério da Agricultura, Pecuária e Abastecimento, Brazil**. Disponível em: <https://www.gov.br/agricultura/pt-br/assuntos/sanidade-animal-e-vegetal/saude-animal/programas-de-saude-animal/brucelose-e-tuberculose/principais-normas-pncebt/in-10-de-3-de-marco-de-2017-aprova-o-regulamento-tecnico-do-pncebt.pdf/view>. Acesso em: 17 ago. 2020.

MARINO, S. et al. A methodology for performing global uncertainty and sensitivity analysis in systems biology. **Journal of Theoretical Biology**, v. 254, n. 1, p. 178–196, set. 2008. Disponível em: <http://www.sciencedirect.com/science/article/pii/S0022519308001896>.

MEKONNEN, G. A. et al. Network analysis of dairy cattle movement and associations with bovine tuberculosis spread and control in emerging dairy belts of Ethiopia. **BMC Veterinary Research**, v. 15, n. 1, p. 262, 2019. Disponível em: <https://doi.org/10.1186/s12917-019-1962-1>.

MOSLONKA-LEFEBVRE, M. et al. Market analyses of livestock trade networks to inform the prevention of joint economic and epidemiological risks. **Journal of the Royal Society Interface**, v. 13, n. 116, p. 20151099, 22 mar. 2016. Disponível em: <http://www.ncbi.nlm.nih.gov/pmc/articles/PMC4843675/>.

MOTTA, P. et al. Implications of the cattle trade network in Cameroon for regional disease prevention and control. **Scientific Reports**, v. 7, n. 1, p. 43932, 7 abr. 2017. Disponível em: <http://dx.doi.org/10.1038/srep43932>.

MOUSTAKAS, A. Spatio-temporal data mining in ecological and veterinary epidemiology. **Stochastic Environmental Research and Risk Assessment**, v. 31, n. 4, p. 829–834, 9 maio 2017. Disponível em: <https://doi.org/10.1007/s00477-016-1374-8>.

NABI, K. N. Forecasting COVID-19 pandemic: A data-driven analysis. **Chaos, Solitons & Fractals**, v. 139, p. 110046, out. 2020. Disponível em: <http://www.sciencedirect.com/science/article/pii/S0960077920304434>.

NATALE, F. et al. Network analysis of Italian cattle trade patterns and evaluation of risks for potential disease spread. **Preventive Veterinary Medicine**, v. 92, n. 4, p. 341–350, 2009.

NEPUSZ, G. C. and T. The igraph software package for complex network research. **InterJournal**, v. Complex Sy, p. 1695, 2006. Disponível em: <http://igraph.org>.

O'HARE, A. et al. Estimating epidemiological parameters for bovine tuberculosis in British cattle using a Bayesian partial-likelihood approach. **Proceedings of the Royal Society B: Biological Sciences**, v. 281, n. 1783, p. 20140248, 22 maio 2014.

Disponível em: <https://doi.org/10.1098/rspb.2014.0248>.

ORTIZ-PELAEZ, A. et al. Use of social network analysis to characterize the pattern of animal movements in the initial phases of the 2001 foot and mouth disease (FMD) epidemic in the UK. **Preventive Veterinary Medicine**, v. 76, n. 1–2, p. 40–55, set. 2006. Disponível em: <http://www.sciencedirect.com/science/article/pii/S0167587706000808>.

PALISSON, A.; COURCOUL, A.; DURAND, B. Role of Cattle Movements in Bovine Tuberculosis Spread in France between 2005 and 2014. **PLOS ONE**, v. 11, n. 3, p. e0152578, 28 mar. 2016. Disponível em: <https://doi.org/10.1371/journal.pone.0152578>.

PAYEN, A.; TABOURIER, L.; LATAPY, M. Spreading dynamics in a cattle trade network: Size, speed, typical profile and consequences on epidemic control strategies. **PLOS ONE**, v. 14, n. 6, p. e0217972, 10 jun. 2019. Disponível em: <https://doi.org/10.1371/journal.pone.0217972>.

PEBESMA, E. Simple Features for R: Standardized Support for Spatial Vector Data. **The R Journal**, v. 10, n. 1, p. 439, 2018. Disponível em: <https://journal.r-project.org/archive/2018/RJ-2018-009/index.html>.

PEREZ, A. M. et al. Simulation model of within-herd transmission of bovine tuberculosis in Argentine dairy herds. **Preventive Veterinary Medicine**, v. 54, n. 4, p. 361–372, ago. 2002. Disponível em: <http://www.sciencedirect.com/science/article/pii/S0167587702000430>.

PICASSO-RISSO, C. et al. Modeling the effect of test-and-slaughter strategies to control bovine tuberculosis in endemic high prevalence herds. **Transboundary and Emerging Diseases**, v. n/a, n. n/a, p. tbed.13774, 7 ago. 2020. Disponível em: <https://doi.org/10.1111/tbed.13774>.

POZO, P. et al. Analysis of the cattle movement network and its association with the risk of bovine tuberculosis at the farm level in Castilla y Leon, Spain. **Transboundary and Emerging Diseases**, v. 66, n. 1, p. 327–340, 16 jan. 2019. Disponível em: <https://doi.org/10.1111/tbed.13025>.

PRADO SIQUEIRA, R. **brazilmaps: Brazilian Maps from Different Geographic**

Levels, 2017. . Disponível em: <https://cran.r-project.org/package=brazilmaps>.

QUEIROZ, M. R. et al. Epidemiological status of bovine tuberculosis in the State of Rio Grande do Sul, Brazil. **Semina: Ciências Agrárias**, v. 37, n. 5Supl2, p. 3647, 9 nov. 2016. Disponível em: <http://www.uel.br/revistas/uel/index.php/semagrarias/article/view/27281>. Acesso em: 5 maio. 2017.

R CORE TEAM. **R: A language and environment for statistical computing**Vienna, Austria, AustriaR fundation for Statistical Computing, , 2017. . Disponível em: <https://www.r-project.org>.

RODRIGUES, R. A. et al. False-negative reactions to the comparative intradermal tuberculin test for bovine tuberculosis. **Pesquisa Veterinária Brasileira**, v. 37, n. 12, p. 1380–1384, dez. 2017. Disponível em: <http://www.scielo.br/scielo.php?script=sci_arttext&pid=S0100-736X2017001201380&lng=en&tlng=en>.

ROSE, H.; WALL, R. Modelling the impact of climate change on spatial patterns of disease risk: Sheep blowfly strike by Lucilia sericata in Great Britain. **International Journal for Parasitology**, v. 41, n. 7, p. 739–746, jun. 2011. Disponível em: <http://www.sciencedirect.com/science/article/pii/S0020751911000725>.

SANTOS, D. V. dos et al. Identification of foot and mouth disease risk areas using a multi-criteria analysis approach. **PLOS ONE**, v. 12, n. 5, p. e0178464, 26 maio 2017. Disponível em: <https://doi.org/10.1371/journal.pone.0178464>.

SAVINI, L. et al. Development of a forecasting model for brucellosis spreading in the Italian cattle trade network aimed to prioritise the field interventions. **PLOS ONE**, v. 12, n. 6, p. e0177313, 27 jun. 2017. Disponível em: <https://doi.org/10.1371/journal.pone.0177313>.

SMITH, R. L. et al. Development of a Model to Simulate Infection Dynamics of Mycobacterium Bovis in Cattle Herds in the United States. **Journal of the American Veterinary Medical Association**, v. 243, n. 3, p. 411–423, 1 ago. 2013. Disponível em: <https://pubmed.ncbi.nlm.nih.gov/23865885>.

VANDERWAAL, K. et al. Evaluating empirical contact networks as potential

transmission pathways for infectious diseases. **Journal of The Royal Society Interface**, v. 13, n. 121, p. 20160166, 3 ago. 2016. Disponível em: <http://rsif.royalsocietypublishing.org/lookup/doi/10.1098/rsif.2016.0166>.

VANDERWAAL, K. et al. Optimal surveillance strategies for bovine tuberculosis in a low-prevalence country. **Scientific Reports**, v. 7, n. 1, p. 4140, 2017a. Disponível em: <https://doi.org/10.1038/s41598-017-04466-2>.

VANDERWAAL, K. et al. Translating Big Data into Smart Data for Veterinary Epidemiology. **Frontiers in Veterinary Science**, v. 4, p. 110, 17 jul. 2017b. Disponível em: <https://www.frontiersin.org/article/10.3389/fvets.2017.00110>.

VERTERAMO CHIU, L. J. et al. Assessment of the bovine tuberculosis elimination protocol in the United States. **Journal of Dairy Science**, v. 102, n. 3, p. 2384–2400, mar. 2019. Disponível em: <http://www.sciencedirect.com/science/article/pii/S0022030219300761>.

WASSERMAN, S.; FAUST, K. **Social Network Analysis: Methods and Applications**. [s.l.] Cambridge University Press, 1994.

WICKHAM, H. et al. Welcome to the Tidyverse. **Journal of Open Source Software**, v. 4, n. 43, p. 1686, 21 nov. 2019. Disponível em: <https://joss.theoj.org/papers/10.21105/joss.01686>.

WIDGREN, S. et al. Siminf: An R package for data-driven stochastic disease spread simulations. **Journal of Statistical Software**, 2019.

WILLEBERG, P. W. et al. **The Herd-Level Sensitivity of Abattoir Surveillance for Bovine Tuberculosis: Simulating the Effects of Current and Potentially Modified Meat Inspection Procedures in Irish CattleFrontiers in Veterinary Science**, 2018. . Disponível em: <https://www.frontiersin.org/article/10.3389/fvets.2018.00082>.

YANG, Y. et al. Tuberculosis with relapse: A model. **Mathematical Population Studies**, v. 24, n. 1, p. 3–20, 2 jan. 2017. Disponível em: <https://doi.org/10.1080/08898480.2014.998550>.

Supplementary material

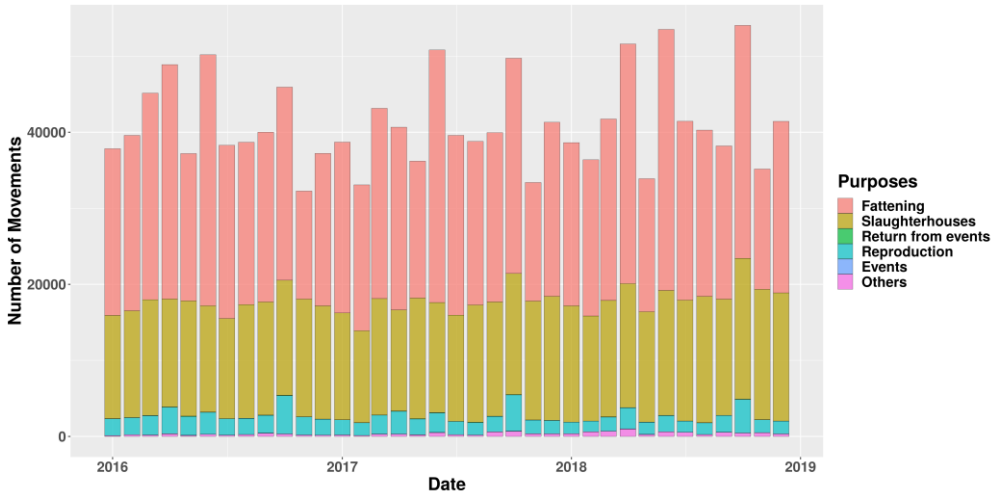

Supplementary figure 1. monthly number of outgoing movements by the declared purposed from all study period in RS state, Brazil.

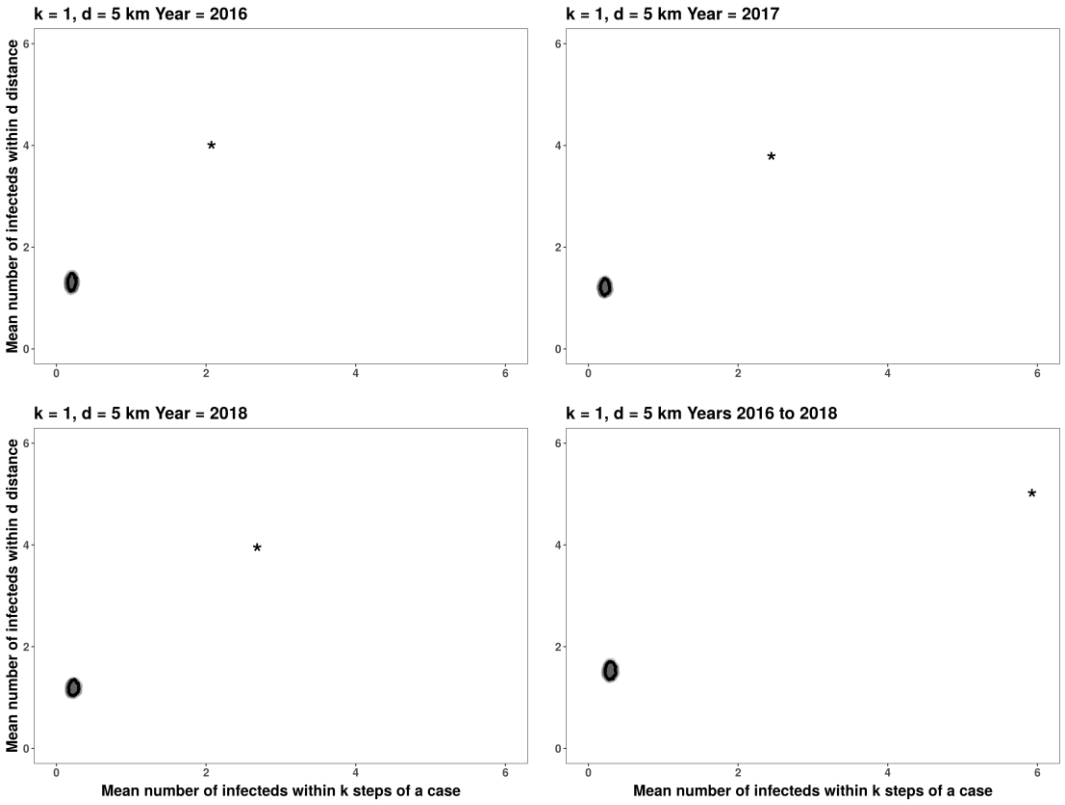

Supplementary figure 2. Graphical results of the k-test. The grey-shaded region in the graph represents the null distribution of the k-statistic when positive premises were randomly distributed within the network. Bold line represents the 95% of the distribution of positive premises within 1 step. The star indicates the observed mean of positive premises within 1 step in the network (x-axis) and positive premises within 5 km (y-axis).

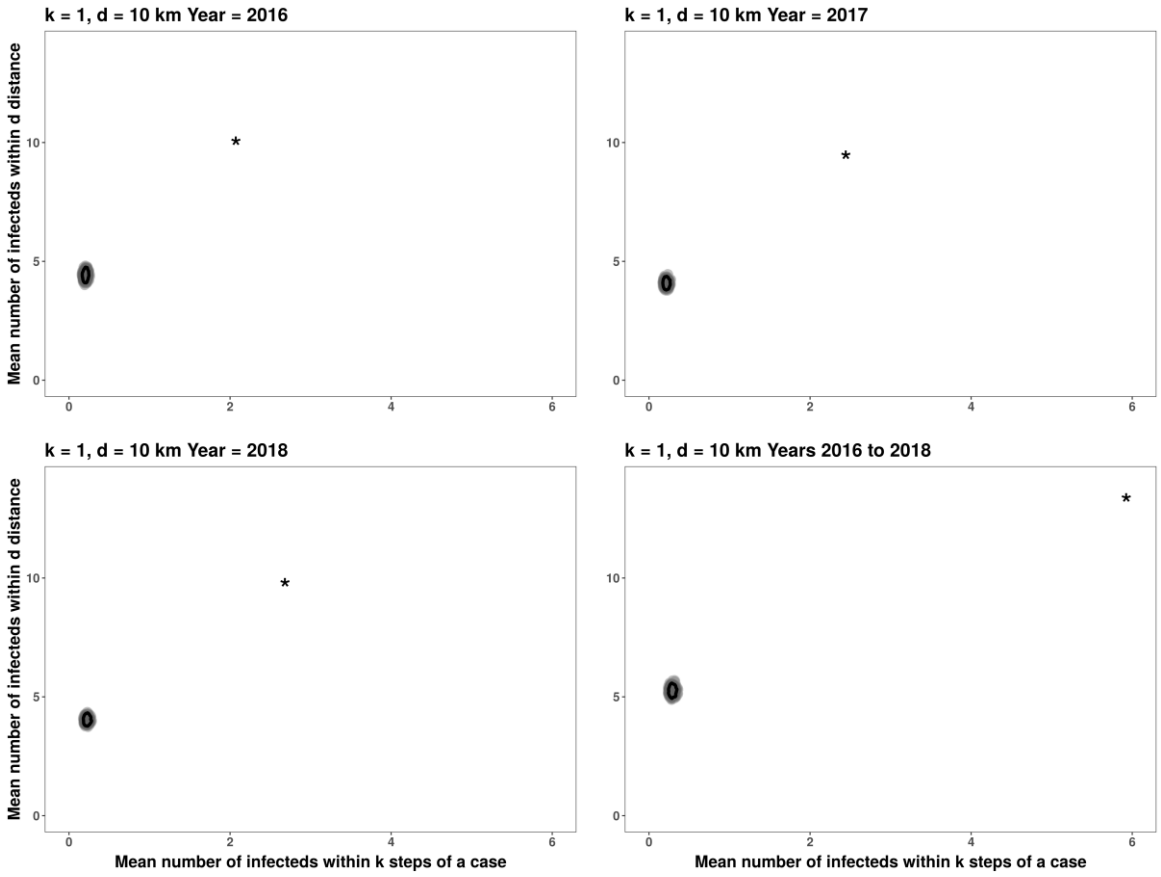

Supplementary figure 3. Graphical results of the k-test. The grey-shaded region in the graph represents the null distribution of the k-statistic when positive premises were randomly distributed within the network. Bold line represents the 95% of the distribution of positive premises within 1 step. The star indicates the value of observed mean of positive Premises within 1 step in the network (x-axis) and positive premises within 10 km (y-axis).

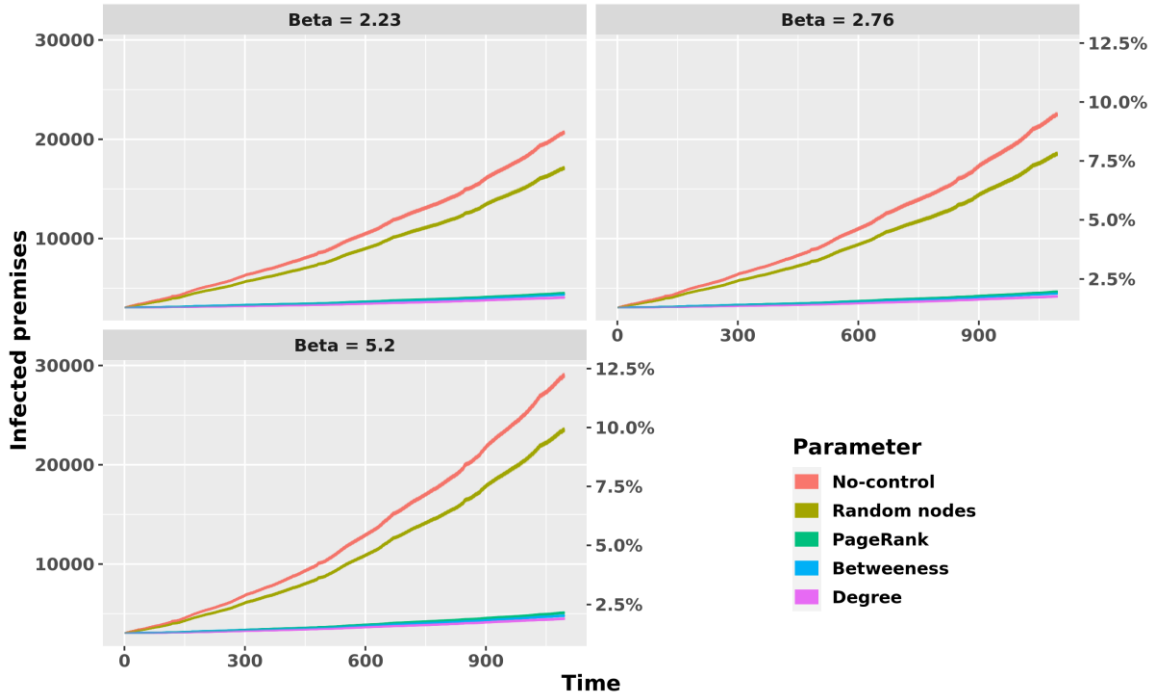

Supplementary figure 4. Infection curves controlling by network-based control actions and without control action (No-control) in the temporal network representation of cattle movements for different probabilities of transmission (1, 2.76 and, 4.13) using TLL positive premises from 2016 to 2017 as initial infected premises. The y-left axis represents the total of infected premises at the end of simulation, and the Y-right represent the percentage of infected premises. The x-axis represents the simulation time in days.

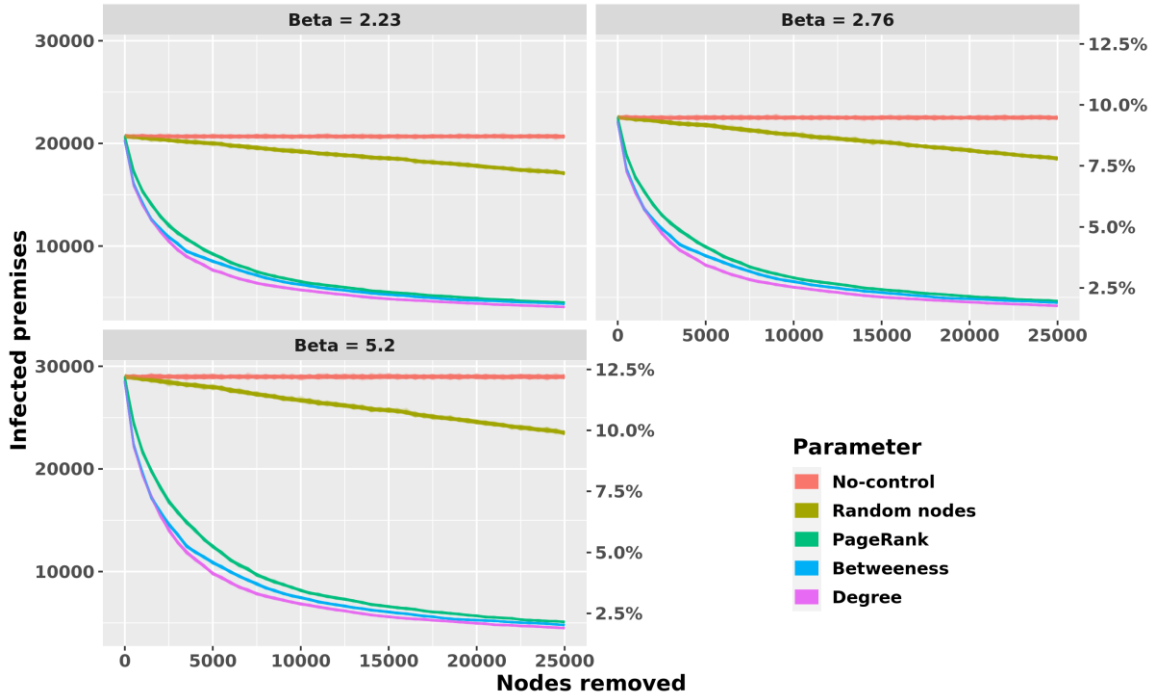

Supplementary figure 5. Node removal model in RS state based on the transmission rates (1, 2.76 and, 4.13) and network parameters: PageRank, betweennesses degree, and random nodes from 10 model interaction using 3,050 TLL positive nodes as initial infected premises in each simulation. The Y- left axis represents the total of infected premises at the end of simulation, and the Y-right represent the percentage of infected premises. The x-axis represents the simulation time in days.

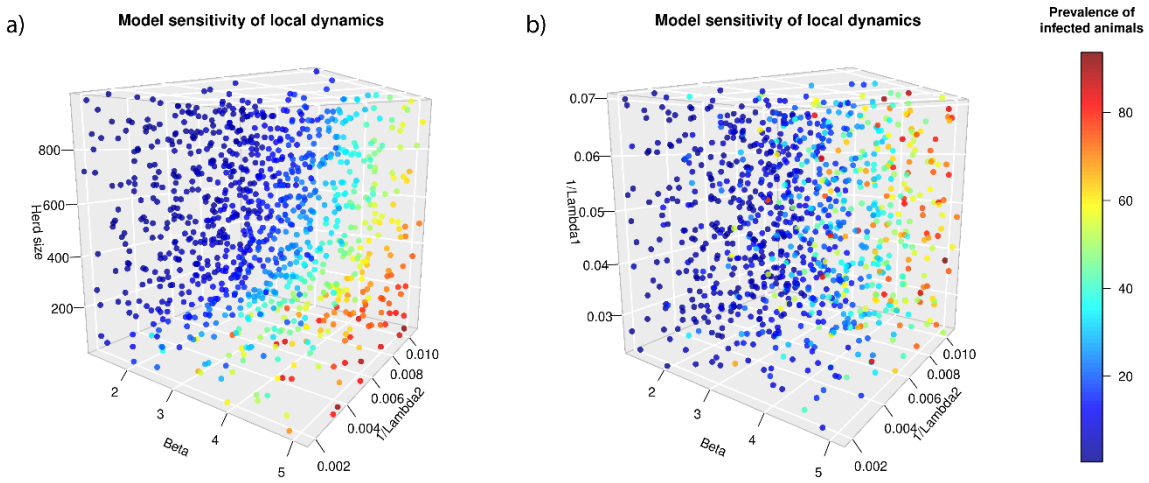

Supplementary figure 6. a) Local sensitivity analysis, dots color represent the mean of prevalence in the stochastic outputs model by the parameters Herd size, beta (β), and 1/lambda 2 ($1/\lambda_2$)**;** b) Local sensitivity analysis, dots color represent the mean of prevalence in the stochastic outputs model by the parameters 1/lambda 1 ($1/\lambda_1$); beta (β), and 1/lambda 2 ($1/\lambda_2$).

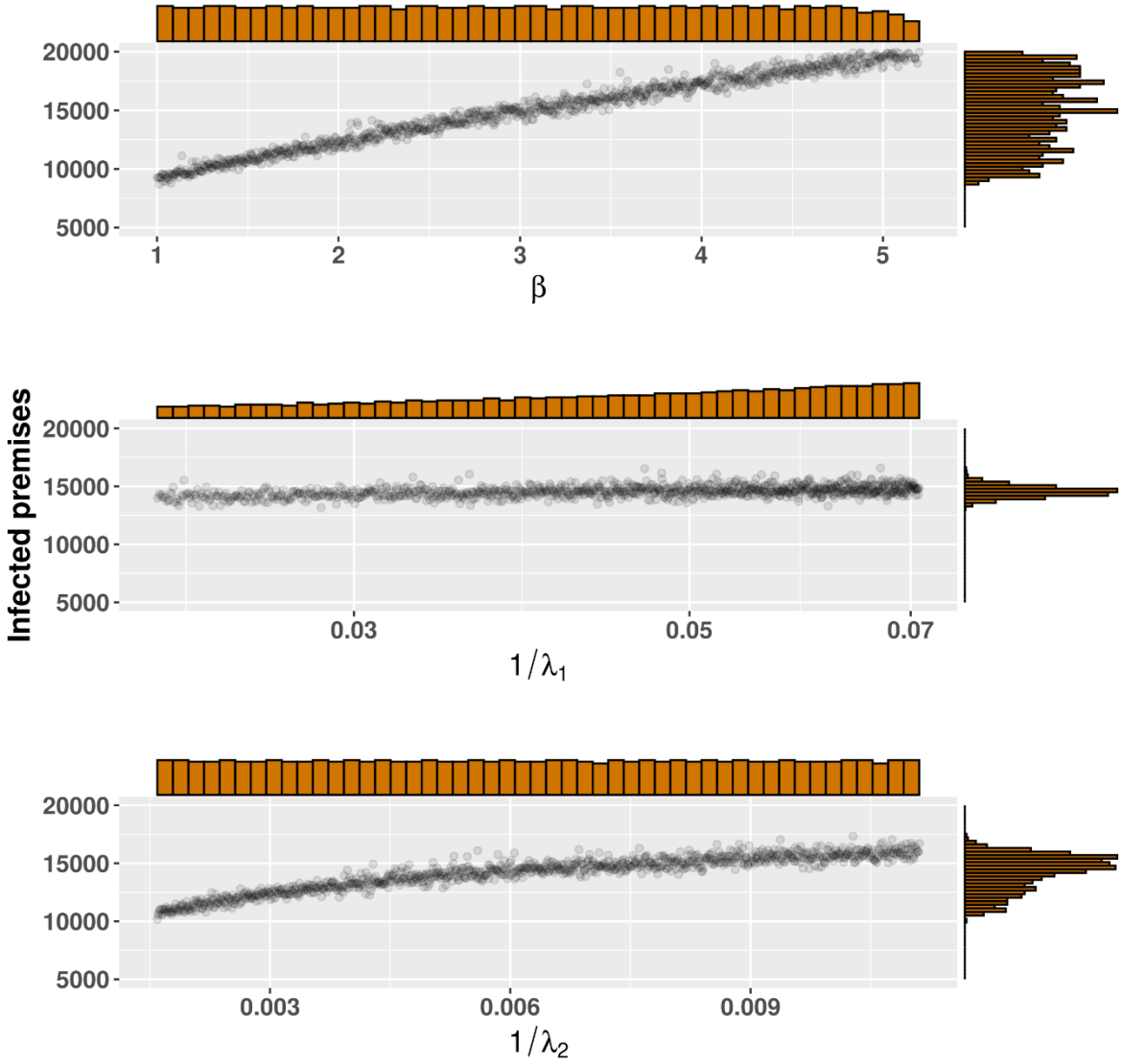

Supplementary figure 7. Global Sensitivity analysis by parameters. Each dot represents one simulation of 1000 for the different parameter values (β, λ_1, and λ_2), marginal plots represents the histograms of each parameter distribution.

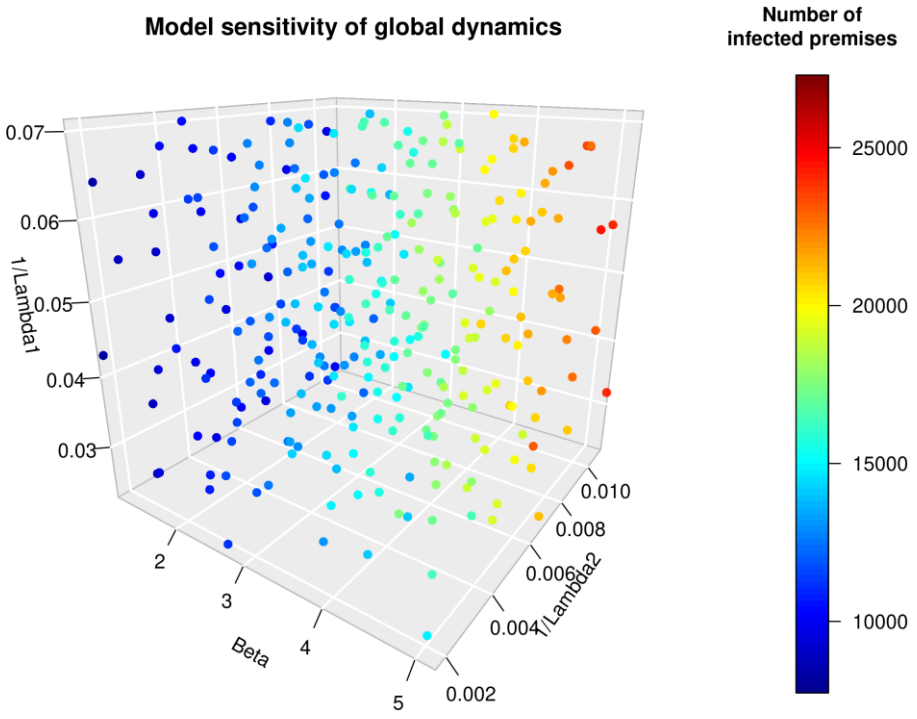

Supplementary figure 8. Model sensitivity of global dynamics analysis, dots color represents the mean of infected premises in the stochastic outputs model by the parameters 1/lambda 1 ($1/\lambda_1$); beta (β), and 1/lambda 2 ($1/\lambda_2$).

Permutation network sensitivity analysis

In order to access to the robust of the model the contact network was permuted 1000 times, to maintain the degree distribution from the permuted network, the births and death (slaughterhouse animals) were preserved and the number of animals in each premise were recalculated according with their specific in/out going movements.

For each permuted network were performed a SORI model (detailed in the material and methods section) and summarized the number of infected premises at the end of the simulation.

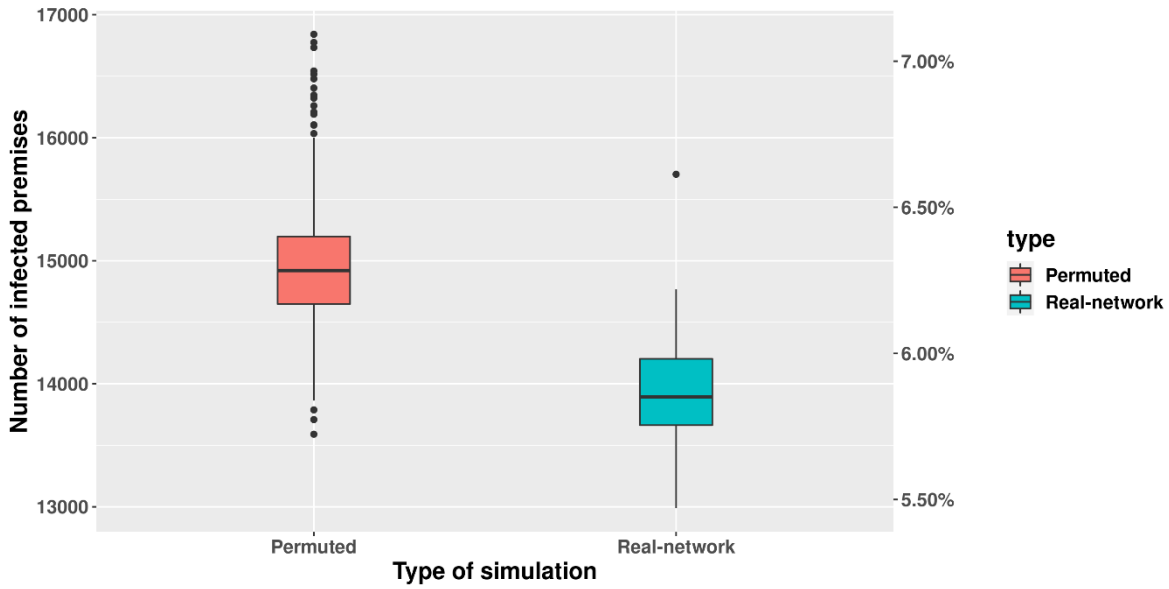

Supplementary figure 9. Global permutation sensitivity analysis, between the permuted networks and the real data network.